

INFORMATION TO USERS

This manuscript has been reproduced from the microfilm master. UMI films the text directly from the original or copy submitted. Thus, some thesis and dissertation copies are in typewriter face, while others may be from any type of computer printer.

The quality of this reproduction is dependent upon the quality of the copy submitted. Broken or indistinct print, colored or poor quality illustrations and photographs, print bleedthrough, substandard margins, and improper alignment can adversely affect reproduction.

In the unlikely event that the author did not send UMI a complete manuscript and there are missing pages, these will be noted. Also, if unauthorized copyright material had to be removed, a note will indicate the deletion.

Oversize materials (e.g., maps, drawings, charts) are reproduced by sectioning the original, beginning at the upper left-hand corner and continuing from left to right in equal sections with small overlaps. Each original is also photographed in one exposure and is included in reduced form at the back of the book.

Photographs included in the original manuscript have been reproduced xerographically in this copy. Higher quality 6" x 9" black and white photographic prints are available for any photographs or illustrations appearing in this copy for an additional charge. Contact UMI directly to order.

UMI

A Bell & Howell Information Company
300 North Zeeb Road, Ann Arbor MI 48106-1346 USA
313/761-4700 800/521-0600

University of Alberta

**Geochemical and Isotopic Study of Granites From Taltson
Magmatic Zone, NE Alberta: Implications For Early Proterozoic
Tectonics in the Western North American craton.**

by
Suman Kumar De



A thesis submitted to the Faculty of Graduate Studies and Research in partial
fulfillment of the requirements for the degree of Master of Science.

Department of Earth and Atmospheric Sciences
Fall 1998.



National Library
of Canada

Acquisitions and
Bibliographic Services

395 Wellington Street
Ottawa ON K1A 0N4
Canada

Bibliothèque nationale
du Canada

Acquisitions et
services bibliographiques

395, rue Wellington
Ottawa ON K1A 0N4
Canada

Your file *Votre référence*

Our file *Notre référence*

The author has granted a non-exclusive licence allowing the National Library of Canada to reproduce, loan, distribute or sell copies of this thesis in microform, paper or electronic formats.

The author retains ownership of the copyright in this thesis. Neither the thesis nor substantial extracts from it may be printed or otherwise reproduced without the author's permission.

L'auteur a accordé une licence non exclusive permettant à la Bibliothèque nationale du Canada de reproduire, prêter, distribuer ou vendre des copies de cette thèse sous la forme de microfiche/film, de reproduction sur papier ou sur format électronique.

L'auteur conserve la propriété du droit d'auteur qui protège cette thèse. Ni la thèse ni des extraits substantiels de celle-ci ne doivent être imprimés ou autrement reproduits sans son autorisation.

0-612-34350-2

University of Alberta

Library Release Form

Name of Author: Suman Kumar De

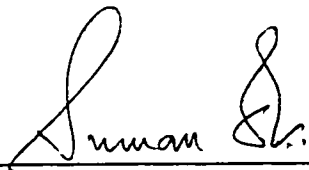
Title of Thesis: Geochemical and Isotopic study of Granites From Taltson Magmatic Zone, NE Alberta: Implications for Early Proterozoic Tectonics in the Western North American Craton.

Degree: Master of Science.

Year this Degree Granted: 1998.

Permission is hereby granted to the University of Alberta Library to reproduce single copies of this thesis and to lend or sell such copies for private, scholarly, or scientific research purposes only.

The author reserves all other publication and other rights in association with the copyright in the thesis, and except as hereinbefore provided, neither the thesis nor any substantial portion thereof may be printed or otherwise reproduced in any material form whatever without the author's prior written permission.



Department of Earth and Atmospheric Sciences.

University of Alberta

Edmonton, Alberta.

CANADA T6G 2E3.

August 14th 1998

University of Alberta

Faculty of Graduate Studies and Research

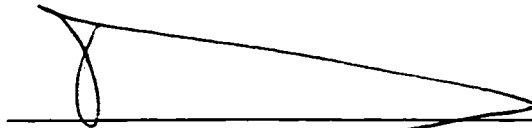
The undersigned certify that they have read, and recommend to the Faculty of Graduate Studies and Research for acceptance, a thesis entitled Isotopic study of Taltson Magmatic Zone Granites, N.E. Alberta: Implications for the Tectonic setting of the Taltson Magmatic Zone in partial fulfillment of the requirements for the degree of Master of Science.



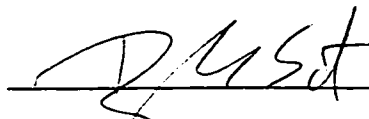
Dr. Thomas Chacko.(Supervisor)



Dr. Robert A. Creaser. (Committee Member)



Dr.Karlis Muehlenbachs. (Committee Member)



Dr. Doug R. Schmitt. (Committee Member)

Date:

August 14, 1998

Abstract

The early Proterozoic Taltson Magmatic Zone (TMZ) comprises the southern part of the Taltson-Thelon orogenic belt. The TMZ is dominated by earlier I-type and later S-type suites of granitoids. Previous workers ascribed the formation of the I-type granitoids to subduction of oceanic crust beneath the Churchill craton in an Andean setting, followed by generation of S-type granitoids during collision between the Churchill craton and the Buffalo Head terrane. Geochemical and isotopic data obtained in this study indicates that the I-type granites of the southern TMZ had an intra-crustal origin which is unlike magmas generated at modern-day Andean margins where a significant mantle contribution to magmatism is recognized. This contradicts the existing tectonic model for the TMZ. We propose that TMZ magmas formed in a tectonic environment similar to the Cordilleran interior of western North America and the Tien Shan area of central Asia where crustal thickening and associated intra-crustal magmatism occur inboard from a convergent plate margin.

Dedicated in memory of my grandfather and to all the people who never had the money or opportunity to go through higher university education.

Acknowledgements

There is never adequate space for writing acknowledgements. I take this opportunity to acknowledge most of my friends and colleagues for encouraging me to bear through this thesis. Funding was provided by an NSERC grants to my supervisor Dr. Tom Chacko, Geological Society of America, 1995 Student Research Award, and University of Alberta, Walter Jones Graduate Student Award to me. I would like to thank Dr. M. McDonough, formerly in Geological Survey of Canada, Calgary and Dr.H.Baadsgaard, University of Alberta for providing me with some samples and his unpublished Nd analyses for this project. Blaine Carlson, pilot of Loon Air, Ft. Smith, Alberta was instrumental in helping me doing my fieldwork.

Dr. Robert Creaser and my friend Katsuyuki Yamashita introduced me into the fascinating world of radiogenic isotopes, and giving me a hands on experience for the endless hours in the laboratory. Dr. Karlis Muehlenbachs introduced me into the field of stable isotope geochemistry and stimulated my mind with his philosophy. James Farquhar made me learn and understand the philosophy behind doing good experiments, and rectified my mistakes over and over again.

I take this opportunity to acknowledge my colleagues Leslie Driver, Rajeev Nair, Matt Perks for their support in every aspect of this work. This work has benefited from stimulating discussions with my friends like Bjarni Gautason, Paul Blanchon, Jochen Mezger, Ram Maikala, Moin Mala, Srinivas, Indranil Barman, Dipanjan Bannerjee, Jimmy Jim Jim, Tracy Kutash, Myrna Salloum and lot of others, as the list of names progressively increases in length. Thank you all.

My present and former room-mates (Paul, David, Scott), my friends like Kevin Brett (special thanks for going through my thesis draft and numerous practice sessions of my talk), Murray Gingras, Branislava Milic, Mikel Erquiaga, Isabell Benton helped me by patiently listening through my stupid comments on cold winter nights. I am glad that my former supervisor Dr. Abhijit Bhattacharrya and mentor like Sabyasachi Sen taught me how not to quit research. Finally I would like to mention that my supervisor Tom Chacko helped me read, write, eat, sleep and financially funded everything for this work to be completed. He also helped me to understand the art of scientific writing and simple logical thinking. Thank you Tom for everything.

Finally I would like to thank my sister, parents, Anirban Sen, Soma Chakraborty for their moral support over these years.

Table of Contents

Introduction	1
Regional Geology	3
Previous Isotopic and Geochemical work	5
Analytical Procedure	6
Results	8
<i>Geochemistry</i>	8
<i>Neodymium, Lead and Oxygen isotopes</i>	10
Discussion	12
<i>Neodymium isotopes</i>	12
<i>Lead isotopes</i>	14
<i>Oxygen isotopes</i>	17
<i>Assimilation and fractional crystallisation</i>	18
<i>Comparison with Phanerozoic continental margin magmatism</i>	19
<i>Towards an alternate tectonic model</i>	22
<i>Implications for the assembly of the North American craton</i>	24
Conclusions	26
References	55
Appendix A	68
Appendix B	69

List of Figures

Figure	Page
1. Geological map showing the tectonic elements of the Western Canadian Shield.	36
2. Geological map of southern Taltson Magmatic Zone with sample locations.	37
3. IUGS classification of granitoids from TMZ	38
4. Harker variation diagrams	39
5. Rare earth element diagrams for the Colin, Wylie and Slave granites.	40
6. Rare earth element diagrams for the Arch Lake granites, metasediments and basement gneisses.	41
7. Pearce element type plots for the TMZ granites.	42
8. ϵ Nd versus Time plot for the western TMZ granites.	43
9. ϵ Nd versus Time plot for the eastern TMZ granites.	44
10. $^{207}\text{Pb}/^{204}\text{Pb}$ versus $^{206}\text{Pb}/^{204}\text{Pb}$ for progressive stages of leaching.	45
11. $^{207}\text{Pb}/^{204}\text{Pb}$ versus $^{206}\text{Pb}/^{204}\text{Pb}$ diagram for TMZ granites.	46
12. Nd-Pb mixing diagram for the Eastern plutons.	47
13. Histograms of oxygen isotopic composition of Eastern and Western TMZ granites, metasediments, and basement gneisses.	48
14. Assimilation fractional crystallisation plot for the Eastern plutons.	49
15. $^{143}\text{Nd}/^{144}\text{Nd}$ versus $\delta^{18}\text{O}$ for Andean calc-alkaline volcanics.	50
16. $^{143}\text{Nd}/^{144}\text{Nd}$ versus $\delta^{18}\text{O}$ for TMZ granites.	51
17. Comparative histograms of oxygen isotopic compositions of plutonic and volcanic rocks from TMZ and CVZ.	52
18. Schematic diagram of Sm-Nd isotopic system	53
19. Schematic diagram for Common Pb isotopic system and range of $\delta^{18}\text{O}$ values for common rock types	54

List of abbreviations

AFC	Assimilation-fractional crystallization
ALSZ	Andrew Lake shear zone
ASI	Alumina saturation index
CLSZ	Charles Lake shear zone
CVZ	Central Volcanic Zone
Ga	10^9 years
HDEHP	Di (2-ethylhexyl) orthophosphoric acid
HEPA	High-efficiency particulate
I-type	Igneous type.
ICP-MS	Inductively Coupled Plasma Mass Spectrometry
LLSZ	Leland Lake shear zone
Ma	10^6 years
REE	Rare earth element
S- type	Sedimentary type
TBC	Taltson Basement Complex
TMZ	Taltson Magmatic Zone
WPG	Within-plate granitoids
VAG	Volcanic-arc granitoids
XRF	X-ray Fluorescence
syncol	Syn-collisional granites

INTRODUCTION

The Earth experienced a major period of continental crust generation and assembly from 2.0-1.6 Ga (e.g., Hoffman, 1988; Windley, 1992; Rogers, 1993; Condie, 1997). Two broad types of orogenesis occurred during this period (Windley, 1992; Patchett, 1992). The first type resulted from the collision of two or more Archean microcontinents and primarily involved recycling of pre-existing continental material. The second type involved the production and amalgamation of large amounts of new continental crust. This typically occurred by the accretion of juvenile island arcs and various intra-oceanic deposits onto the margins of Archean cratons. The Taltson Magmatic Zone (TMZ) of northwestern Canada is an early Proterozoic (2.0-1.9 Ga) orogenic belt that is intermediate between these two end members (Fig.1). The tectonic model proposed for the TMZ involves early subduction of oceanic crust beneath the Archean Churchill province in an Andean-type setting followed by collision between the Churchill and 2.0-2.4 Ga Buffalo Head Terrane (Hoffman, 1988, 1989; Ross et al., 1991 Theriault and Ross, 1991; McDonough et al., 1993; 1995). A similar tectonic model has been proposed for the Thelon orogen, the northward extension of the TMZ (Hoffman, 1987; 1988). A major line of evidence used to support these models is the petrological, geochemical or isotopic character of granitic rocks occurring in the Taltson-Thelon orogenic belt. More specifically, the early (1.96-2.0 Ga) I-type granite suite of the belt is attributed to the subduction phase of orogenesis and the voluminous S-type suite to the subsequent collisional event (Hoffman, 1988; Theriault, 1992; McDonough, 1994; 1995).

The aim of the present study is to examine the geochemical and isotopic character of TMZ granites in greater detail with a view to understanding better the tectonic environment in which these rocks formed. This work builds on earlier geological, geochemical and isotopic studies in the TMZ (Godfrey, 1986; Bostock et al., 1987; Goff

et al., 1986; Theriault and Bostock, 1989; Theriault & Ross 1991; Theriault, 1992; McDonough et al., 1994; 1995). Unlike the earlier studies, however, we make use of a multiple isotope approach (Nd, Pb, and O). Studies in other areas have shown that such an approach provides a more comprehensive picture of granite petrogenesis than studies depending on a single geochemical or isotopic parameter (e.g., James, 1982; Taylor, 1986; Whalen et al., 1994). For example, neodymium and lead isotope data are useful in determining the relative proportions of crust and mantle involvement in the generation of granitic magmas. These isotopic systems also provide two independent estimates of the average age of the granite source regions. The oxygen isotope system provides different information on the source characteristics. In particular, it provides information on the contribution of supracrustal material to the granitic magmas. The combined use of stable and radiogenic isotopic studies provides a means of constraining the nature and age of different source materials and estimating the relative contribution of crust and mantle to the granitic magmas. This in turn helps to decipher the tectonic setting in which the granites originated.

In this study, we examine both I- and S-type granite suites from the southern part of the TMZ. We show that the early I-type granites are unlike magmas generated at modern-day Andean-type margins where a significant mantle contribution to magmatism is easily recognized. Instead, the petrological, geochemical and isotopic data point to an intra-crustal origin for the early granites. This raises serious questions about the validity of the existing tectonic model as it applies to the southern segment of the TMZ. Data on the later S-type granites indicate that they were derived from the melting of pelitic metasediments, consistent with the findings of earlier studies (Theriault, 1992; Chacko et al., 1994; 1995; Creaser, 1995). On the basis of our data, we propose an alternative tectonic model that better accounts for the nature of magmatic activity in the TMZ.

REGIONAL GEOLOGY

The Taltson Magmatic Zone (TMZ) of northeastern Alberta makes up the southern part of the 2500 km long Taltson-Thelon (2.0-1.9 Ga) orogenic belt (Hoffman 1988, 1989). The TMZ is bounded on the west by the 2.0-2.4 Ga Buffalo Head Terrane and on the east by the Archean Churchill Province (Fig. 1) (Ross et al., 1991). The 300 km exposed section of the TMZ in Alberta and the Northwest Territories comprises granitoids, metasedimentary gneisses, granitic basement gneisses and amphibolites.

Geological and geochronological studies in the Precambrian shield of northeastern Alberta, which includes the TMZ, began more than three decades ago (Godfrey, 1961; 1963; 1986; Baadsgaard and Godfrey, 1967; 1972). These pioneering studies served as the foundation for later structural, petrological, geochemical and isotopic studies in the area (Godfrey and Langenberg, 1978; Nielsen et al., 1981; Langenberg and Nielsen, 1982; Goff et al., 1986; McDonough et al., 1994, 1995). Work has also focussed on the northward extension of the TMZ into the Northwest Territories (Bostock et al., 1987; 1988; 1991; Theriault, 1992). Collectively, these studies have shown that the TMZ is dominated by 1.99 - 1.93 Ga granitoid rocks. These include several earlier suites of biotite, and hornblende-biotite granites and granodiorites; the 1.986 Ga Deskenatlata suite (Bostock et al., 1987), the 1.971 Ga Colin Lake suite (McDonough et al., 1997) and the 1.963 Ga Wylie Lake suite (McDonough et al., 1995). Volumetrically very minor quartz diorites have also been reported from these suites (Bostock et al., 1987; Theriault, 1992; Goff et al., 1986). This early phase of weakly peraluminous to metaluminous magmatism was followed by a large volume of moderately to strongly peraluminous magmatism. The latter include the 1.955-1.933 Ga biotite±garnet±cordierite±spinel granites of the Slave and Konth suites (Bostock et al., 1987; Bostock & Loveridge, 1988; Bostock et al., 1991) and the 1.928 Ga biotite granites of the Arch Lake suite (McNicoll

et al., 1993). The age of the Arch Lake granite is tenuous because these granites are intruded by the 1.933 Ga Slave granite (McDonough et al., 1995).

The present study focuses on granitoids and associated basement rocks of the southern Taltson Magmatic Zone (south of the 60°N parallel). The granitoids of the southern TMZ can be divided into eastern and western groups. The eastern group consists of the biotite and hornblende-biotite granites and granodiorites of the Colin Lake and Wylie Lake suites (Fig 2). The western group of plutons comprises the biotite granites of the Arch Lake suite and biotite±garnet±cordierite±spinel granites of the Slave suite (Fig. 2). The two groups of plutons are separated by a screen of basement rocks referred to as the Taltson Basement Complex [TBC] (McDonough, 1994). The TBC is lithologically diverse, primarily consisting of 2.3 Ga hornblende-biotite gneisses, amphibolites and paragneisses (Bostock & van Breemen, 1994; Theriault 1994). The TMZ also contains numerous bodies of high-grade pelitic metasediments (Goff et al., 1986; McDonough et al., 1995), some of which are also found as enclaves in the Slave suite granites (Chacko & Creaser, 1995; Grover et al., 1997). Bostock and van Breemen (1994) postulated that these metasedimentary rocks are the dismembered remnants of a large sedimentary basin, the Rutledge River Basin, that existed before 2.09 Ga.

The southern TMZ is transected by three major north-south oriented shear zones (McDonough et al., 1993, 1994, 1995). These are the Leland Lake (LLSZ), Charles Lake (CLSZ) and Andrew Lake (ALSZ) shear zones (Godfrey et al., 1978; McDonough et al., 1995). Deformation textures and shear sense indicators indicate a predominantly sinistral sense of shearing at granulite- to upper amphibolite-facies conditions (McDonough et al. 1995). The Colin Lake pluton (1.971 Ga) is moderately foliated and locally intrudes and crosscuts ductile shear zone fabrics in the ALSZ (McDonough et al., 1993). The Wylie Lake pluton (1.963 Ga), lying east of the CLSZ, is moderately to strongly foliated, and shows ductile deformation as the shear zone is approached from the

east (McDonough, 1994). The Arch Lake pluton, which is sandwiched between the LLSZ and CLSZ, consists of ductilely deformed and aligned K-feldspar megacrystic granites. The Slave granite plutons are post-tectonic relative to the granulite-grade mylonite fabrics in the LLSZ. These relationships indicate a range of ages for the shear zones, from greater than 1.971 Ga for ALSZ to greater than 1.933 Ga for LLSZ. These shear zones are interpreted as escape structures for TMZ crust from Slave-Churchill collision (Hoffman, 1987; McDonough et al., 1993; 1995)

PREVIOUS ISOTOPIC AND GEOCHEMICAL WORK

The early and late phases of granitoid magmatism in the TMZ are interpreted to have formed in continental-margin arc and continent-continent collisional settings, respectively (Hoffman, 1988; 1989; Ross et al., 1991; Theriault and Ross, 1991; Theriault, 1992; McDonough et al., 1994; 1995). Of the studies cited above, however, only Theriault (1992) evaluated the link between the magmatism and tectonics in the TMZ in detail. He showed that the early Deskenatlata suite granitoids of the northern TMZ plot in the volcanic arc field on Pearce-element discrimination diagrams. He also showed that these rocks have slightly more juvenile Nd isotope signatures than granitoids of the later Slave and Konth suites. The latter have Nd isotope compositions that completely overlap those of the high-grade metasedimentary rocks from which they are interpreted to be derived. Theriault (1992) interpreted these data to reflect a significant mantle contribution to the Deskenatlata magmas, consistent with the existing tectonic model that these rocks formed during subduction of oceanic crust beneath the western margin of the Churchill craton. The Slave and Konth suites were interpreted to have formed by melting of metasediments during the subsequent collision between the Churchill Craton and the Buffalo Head Terrane.

Theriault's (1992) work focussed on the granitoids of the northern TMZ. Although there exists an extensive petrographic and geochemical database (Goff et al., 1986), no comparable study examining the link between magmatism and tectonics has been undertaken for the granitoids of the southern TMZ. The primary objective of the present study is to evaluate this link in detail.

ANALYTICAL PROCEDURES

Sampling for isotopic work was done by collecting representative samples from each of the granite plutons and the TBC (Fig 2). Sampling was performed mainly by float plane; some samples were provided by Dr. H. Baadsgaard, and two samples of TBC gneiss were provided by Dr. M. McDonough of the Geological Survey of Canada. Most of the granite samples collected were away from the shear zones and the ones showing the least deformation and alteration were selected for isotopic work. A suite of thirty-two granite and basement gneiss samples from the Taltson Magmatic Zone were analyzed for their major- and trace-element, and Nd, Pb and O isotope compositions (Tables 1 - 4). Another set of twenty-one unpublished Nd analyses of granites and basement gneisses was obtained from Dr. H. Baadsgaard, University of Alberta. Samples were crushed to gravel size without contaminating them with a metal surface, followed by final grinding to ~35 μm powder. Major- and trace-element analyses were done at Washington State University by X-Ray Fluorescence (XRF) and Inductively Coupled Plasma Mass Spectrometry (ICP-MS) techniques, respectively (Hooper et al., 1993; Knaack et al., 1994).

For Nd isotope analysis, sample powders were accurately weighed and spiked with mixed ^{149}Sm - ^{150}Nd tracer solution before the acid dissolution, and then passed through cation and HDEHP chromatography column to separate Sm and Nd (see Creaser et al., 1997). The Nd isotope ratios were measured on a five collector VG354 thermal

ionization mass spectrometer in multidynamic peak hopping mode. All Nd isotopic ratios were normalized to $^{146}\text{Nd}/^{144}\text{Nd} = 0.7219$. The value obtained for a spiked aliquot of the La Jolla isotopic standard was 0.511848 (± 8) and the in-house "Nd-oxide" standard gave an external reproducibility of 0.000016 (2σ). All $\epsilon\text{Nd}_{\text{TR}}$ calculations were made using published U-Pb zircon ages for the granites. The estimated error on an individual $\epsilon\text{Nd}_{\text{TR}}$ calculation is ± 0.5 ϵ units. Depleted mantle model ages (T_{DM}) are calculated according to the model of Goldstein (1984).

Alkali feldspar for common Pb analyses were first separated from the crushed whole-rock samples using a TBE-acetone mixture and Frantz isodynamic separator. Mineral separates were then sieved to collect grains that were less than 70 microns. X-Ray Diffraction and optical tests confirmed the purity of the separates. Finally, the grains were handpicked under a binocular microscope to remove any remaining impurities. The samples were ultrasonically cleaned in distilled acetone for approximately ten minutes and rinsed with millipore water before leaching. Approximately 300 to 500 mg of feldspar grains were leached overnight in 2N HCl (L1), 6N HCl (L2), 16N HNO₃ (L3) and 16N HNO₃ + one drop of 48% HF (L4) successively. The final residue was dissolved in 4:1 HF: HNO₃ mixture (Cumming & Krstic 1987). Leachates and residues were dried under laminated flow of HEPA-filtered air, redissolved in 3N HBr and dried before the final dissolution in 0.5N HBr. Pb was extracted using combined HBr and HBr-HNO₃ column chemistry modified after Lugmair and Galer (1992). Total blank for the entire chemical procedure was approximately 150 pg, thus no blank corrections were applied. The samples were loaded with silica gel and H₃PO₄ on a Re filament and isotopic measurements were performed on a Micromass 30 thermal ionization mass spectrometer in single collector mode at 1250°C. Measured isotopic ratios were corrected against the recommended value for NBS 981 by Todt et al. (1996) for mass fractionation ($\sim 0.14\%$

/amu). The external reproducibility of the Pb isotopic analysis were 0.33, 0.47, 0.64 per mil (1σ) for $^{206}\text{Pb}/^{204}\text{Pb}$, $^{207}\text{Pb}/^{204}\text{Pb}$, $^{208}\text{Pb}/^{204}\text{Pb}$, respectively, based on 10 separate analyses of NBS 981.

Oxygen isotope analyses of whole-rock samples and quartz mineral separates were performed at the University of Western Ontario and the University of Alberta. Mineral separates were obtained using conventional techniques (magnetic and density separation) and further purified by handpicking. Purity was checked by XRD and is better than 95% for the mineral separates. Oxygen was extracted from 10-15 mg aliquots for whole rock powders and 5-10mg aliquots for quartz separates and converted to CO_2 using conventional techniques (Clayton & Mayeda; 1963). All $\delta^{18}\text{O}$ values were normalized to the reference NBS-28 quartz standard value of 9.6 ‰.

RESULTS

Geochemistry

The results of the major- and trace-element analyses are given in Table 1. In the normative IUGS classification scheme derived empirically by Streckeisen and LeMaitre (1979). The TMZ rocks classify mainly as granites, granodiorites, with a few quartz monzonites (Fig.3). No tonalites or quartz diorites were found as part of this study nor are these rock types significantly represented in the larger sample base of Goff et al. (1986).

Conventional Harker variation diagrams for major elements are shown in Fig.4. With the exception of K_2O and Na_2O , the concentrations of all major elements decrease with increasing SiO_2 for both western and eastern plutons. There is a distinction between the two groups of plutons in their ranges of SiO_2 ; the eastern plutons range from 63 to 74 wt % SiO_2 whereas the western plutons generally have >70 wt % SiO_2 . The distinction

between the two groups is also reflected in terms of the alumina saturation index (ASI). The western plutons mostly comprise strongly peraluminous granitoids ($ASI > 1.1$), with a few moderately peraluminous samples. In contrast, the eastern plutons comprise mainly metaluminous to moderately peraluminous granites. The difference in ASI values are consistent with the presence of metaluminous mineral, hornblende, in some eastern plutons samples, and the strongly peraluminous minerals, garnet, cordierite and spinel, in some of the western pluton samples. In the classification of granites developed by Chappell and White, (1974), the western and eastern plutons have broadly S- and I-type affinities, respectively.

Chondrite normalized rare earth element (REE) plots for the TMZ granites are shown in Fig 5, 6. The eastern plutons and the Arch Lake granites have steep REE patterns with small to moderate negative Eu anomalies ($Eu/Eu^* = 0.37$ to 0.83). The Slave granites have more variable REE patterns and with both negative and positive Eu anomalies. One noteworthy feature of all the TMZ granitoids is unusually steep REE patterns, with $La_N/Yb_N = 15-70$, compared to typical post-Archean granitoids $La_N/Yb_N = 5-15$ (Martin, 1986). High La_N/Yb_N may reflect the presence of garnet as a residual mineral in the granite source region, which, particularly for I-type source regions, would imply that partial melting took place at the high pressures necessary for garnet stability (Hanson, 1980; Martin, 1986). Alternatively, high La_N/Yb_N could be inherited from a source region possessing this geochemical characteristic. The latter possibility is consistent with the observation that the metasediments and TBC gneisses, potential source rocks for the TMZ granites, also have high La_N/Yb_N (Fig. 6)

Tectonic settings of granitic rocks are commonly interpreted in terms of the discrimination diagrams of Pearce et al. (1984). In such plots (Fig. 7), data for the Slave and Arch plutons are scattered between the syn-collisional and volcanic-arc granite fields. The eastern pluton granites plot exclusively in the field of volcanic-arc granitoids. A

similar result was obtained for the early Deskanatlata suite of granites of northern TMZ (Theriault, 1992) and was one line of evidence used to suggest a subduction-related origin for these rocks. However, as discussed further below, several more compelling lines of evidence indicate that the eastern plutons are not related to continental-arc magmatism.

Neodymium, Lead and Oxygen isotopes

Nd, Pb and oxygen data for the TMZ granites, metasediments and basement gneisses are listed in Tables 2-4. ϵNd values range from -3.4 to -7.3 and from -5.2 to -9.8 for the Slave and Arch Lake granites, respectively. Although the two plutonic suites show some overlap, the Arch Lake granites, on the whole, have more negative ϵNd values. The T_{DM} ages of both suites range from 2.6-3.2 Ga, with most samples between 2.6-2.9 Ga. In terms of their Nd isotope signatures, the Slave and Arch Lake granites of the southern TMZ are similar to their northern TMZ counterparts (Slave and Konth suites). The Colin Lake and Wylie Lake granitoids have essentially identical ranges of ϵNd values from -3.4 to -6.1 and T_{DM} ages (2.6-2.8 Ga). Though geochemically similar to the Deskanatlata suite of the northern TMZ (Theriault, 1992), the southern TMZ suites have a more slightly negative Nd isotope signature than the Deskanatlata granites ($\epsilon\text{Nd} = -2.7$ to -3.6).

Ten samples were analysed from the Taltson Basement Complex (TBC). Their $\epsilon\text{Nd}_{(1.97)}$ values range from -3.1 to -9.8, apart from the sample C233588 which is -17.9. The available basement samples show a wide range of T_{DM} (2.5 to 3.6 Ga) but most have model ages between (2.7 and 2.9 Ga).

The lead isotope composition of separated alkali feldspars from all the granite suites, two metasediments and two basement rocks from the southern TMZ are listed in Table 3. Granite feldspar samples for which both leachates and the residue were analyzed plot close to the 1.97 Ga reference isochron, confirming, within error, that U and Pb in the feldspars behaved as closed systems since the time of crystallization (Fig.10). The leaching procedure is designed to eliminate all of the radiogenic components in feldspars. Minor differences in Pb isotope composition between the residue and the fourth leachate in majority of the samples suggest that the procedure was generally successful and that most of the radiogenic Pb was removed via leaching. Nonetheless, there may be small component of radiogenic lead in the residue and hence the Pb isotopic composition of the residues must be treated as a maximum value for the initial Pb. All the granite samples from the eastern and the western plutons, except the Arch Lake pluton, plot in a tight cluster with $^{206}\text{Pb}/^{204}\text{Pb}$ values of 15.49 to 16.52, $^{207}\text{Pb}/^{204}\text{Pb}$ values of 15.27 to 15.47, and $^{208}\text{Pb}/^{204}\text{Pb}$ values of 35.19 to 35.92. The Arch Lake granites are less radiogenic than the other plutons, with $^{206}\text{Pb}/^{204}\text{Pb}$ values of 15.08 to 15.43, $^{207}\text{Pb}/^{204}\text{Pb}$ values of 15.11 to 15.38, and $^{208}\text{Pb}/^{204}\text{Pb}$ values of 34.9 to 35.32. These data indicate a distinct source or combination of sources for the Arch Lake suite. The metasediments from the TBC have $^{206}\text{Pb}/^{204}\text{Pb}$ values of 15.22 to 15.67, $^{207}\text{Pb}/^{204}\text{Pb}$ values of 15.06 to 15.32, and $^{208}\text{Pb}/^{204}\text{Pb}$ values of 35.06 to 35.17. The leached feldspars of the TBC gneisses have $^{206}\text{Pb}/^{204}\text{Pb}$ values of 14.71 to 15.08, $^{207}\text{Pb}/^{204}\text{Pb}$ values of 15.02 to 15.16, and $^{208}\text{Pb}/^{204}\text{Pb}$ values of 34.84 to 34.94. This wide scattering in the values of the basement samples is probably due to the heterogeneous nature of the TBC and its complex pre- 2.0 Ga history (Bostock and Van Breeman 1994, McDonough et al., 1994; 1995).

The range of whole-rock $\delta^{18}\text{O}$ values for the granites is +8.6 to +11.6‰. The basement gneisses have a range from +7.3 to +8.8‰, which are lower than the metasediments (+9.3 to +10.8‰). In general, the western plutons have higher $\delta^{18}\text{O}$

values (+9.6 to +11.6‰) than the eastern plutons (+8.6 to +9.9‰). One of the eastern pluton samples, TMZ-1, has a higher $\delta^{18}\text{O}$ value (10.8‰). However, this sample is more strongly deformed than the other analyzed samples and shows extensive sericitization of the plagioclase. Thus, it is likely that the elevated ^{18}O content is not a primary igneous feature but reflects some sub-solidus alteration. Oxygen isotope data from quartz mineral separates of two remaining eastern pluton samples indicate approximately normal quartz-whole rock fractionation factors (Taylor and Epstein, 1962). This suggests that there has not been extensive modification of primary $\delta^{18}\text{O}$ values of most of the granite samples.

DISCUSSION

Our primary objective in collecting geochemical and isotopic data for the TMZ granitoids and associated rocks is to gain insight as to the age and petrological character of the granitoid source region. In particular, our aim is to assess the relative contribution of crust versus mantle sources to the granitoid magmas. We follow a sequential procedure to obtain this information, considering in turn Nd, Pb and O isotope data. We then compare data for the TMZ granitoids with available data for more recent continental margin magmatism in the Andes and the Himalayas. This comparison provides a rigorous test of the “subduction followed by collision” tectonic model that has been proposed for the TMZ.

Neodymium isotopes

The neodymium isotopic composition of rocks are conveniently reported in terms of $\epsilon\text{Nd}_{\text{TN}}$ notation (DePaolo, 1980). Granites derived directly from the depleted mantle at 1.94 -1.97 Ga, the age range of the southern TMZ granites, could have $\epsilon\text{Nd}_{\text{TN}}$ values of

+3 to +4 using the Goldstein (1984) model. Granitoids derived from partial melting of continental crust at 1.94 - 1.97 Ga could have a range of $\epsilon\text{Nd}_{\text{cr}}^T$ values, depending on the age and Sm/Nd ratio of the crustal materials. In general, however, crustally-derived granites will have $\epsilon\text{Nd}_{\text{cr}}^T$ values ranging from -3 to below -10 (Patchett, 1986). Granites derived from a combination of mantle and crustal sources will have $\epsilon\text{Nd}_{\text{cr}}^T$ values intermediate between the two extremes.

In light of these general considerations, we evaluate the Nd isotopic composition of the Slave granites and the Arch lake granites of the western TMZ. The $\epsilon\text{Nd}_{\text{cr}}^T$ values range from -3.4 to -9.8 (Fig.8). There is a considerable overlap between the Slave and Arch Lake granites, although, in general, the Arch Lake granites have a more negative $\epsilon\text{Nd}_{\text{cr}}^T$ values. This suggests slightly different source rocks for the Arch Lake granites; specifically a source with a longer crustal residence time or lower Sm/Nd relative to the Slave granite protoliths. The range of $\epsilon\text{Nd}_{\text{cr}}^T$ values determined for the Slave granites overlap those of the metasedimentary rocks analyzed from the TMZ (Creaser unpublished data, present study, Theriault 1992, Creaser 1995). It had been earlier proposed that the S-type granites of the TMZ were derived from partial melting of these metasedimentary source rocks (Theriault 1992; Chacko et. al., 1994; Creaser 1995). This proposal is in full agreement with the Nd isotope data presented here.

The I-type granites of the Colin Lake and Wylie Lake suites have essentially identical ranges of $\epsilon\text{Nd}_{\text{cr}}^T$ values from -3.4 to -6.1 (Fig.9). These values overlap those obtained for gneisses, amphibolites and mafic granulites from the TMZ, and late Archean mafic volcanics from the Churchill craton. This observation is consistent with the idea that the granites are derived entirely from partial melting of such sources. However, as

discussed further below, the Pb isotope compositions of TBC gneisses preclude this possibility.

Lead isotopes

The composition of leached K-feldspar separates from TMZ granitoids and metasediments, and TBC felsic gneisses are shown on a $^{207}\text{Pb}/^{204}\text{Pb} - ^{206}\text{Pb}/^{204}\text{Pb}$ diagram (Fig. 11). We assume that all the data approximate the initial lead isotopic of these rocks at 1.93 - 1.97 Ga, the age of magmatism and high-grade metamorphism in the TMZ. The Pb isotopic composition of Slave granites overlap those of TMZ metasediments which, consistent with all other lines of petrological and isotopic evidence, indicates that these granites were derived from partial melting of these metasediments. The Arch Lake granites and the eastern plutons have less radiogenic Pb isotope compositions than the Slave granites indicative of source regions with a lower time-integrated U/Pb. Neither the Arch Lake nor the eastern pluton data arrays can be produced by melting of solely metasedimentary or gneissic sources. They can, however, be generated by mixing of unradiogenic Pb from TBC felsic gneisses and radiogenic Pb from the metasediments.

It is important to note that mixing of Pb derived from 1.97 Ga mantle (Zartman & Doe, 1981) and TBC gneisses cannot generate any of the data arrays of the TMZ granitoids. In contrast, mixing of mantle and metasediments could broadly produce these arrays. However, consideration of mixing in multiple isotope systems such as Nd vs. Pb demonstrates that this mix would have to consist of more than 90% of the metasedimentary end member (Fig.12). An overwhelming proportion of metasediment in the mix is not consistent with the metaluminous to only moderately peraluminous character of the eastern plutons. This argues against such a mixing process and, in turn,

against a significant mantle contribution to even the most apparently juvenile of the TMZ granitoids.

Linear data arrays on $^{207}\text{Pb}/^{204}\text{Pb}$ vs. $^{206}\text{Pb}/^{204}\text{Pb}$ plots, such as those seen for the TMZ granitoids, have been typically interpreted in one of two ways. First, such arrays have been interpreted as secondary isochrons. That is, the slope of the data array is assumed to be proportional to the time elapsed since the rocks of the granite source region had a uniform Pb isotope composition. A least-squares regression line fitted to all of the analyzed TMZ granite samples has a slope of $0.35 \pm 0.02(2\sigma)$ (Williamson, 1968). Substituted into equation 19.37 of Faure (1986), this slope corresponds to an average of $2.9 \pm 0.1\text{Ga}$ for the granite source region. It is noteworthy that this Pb model age is in reasonable agreement with the average Nd model ages obtained for most of the TMZ granitoids ($T_{\text{DM}} = 2.6 - 2.9\text{ Ga}$)

Alternatively, these types of linear arrays have been attributed to mixing between two isotopically different components. In such cases, the slope of the array is assumed to have no age significance but is simply controlled by the isotopic composition of the two end members involved in the mixing process.

Here, we suggest a third possibility. We believe that the array is indeed produced by mixing between two end members, the metasediments and TBC gneisses. However, unlike the usual case with mixing, we propose the following scenario in which the mixing array would also be a secondary isochron, and, therefore, the slope of this array would have age significance. The erosion of a late Archean gneissic terrane produces sediment with a similar Pb isotope composition but a different U/Pb than its source rock. For example typical Archean gneisses of tonalitic composition have U/Pb values of 0.09 ± 0.02 (Feng et al., 1993, Perks, 1997; Yamashita, 1997; present study), compared to values of 0.16 ± 0.09 for late Archean and early Proterozoic metasediments (Taylor and McLennan, 1985; Feng et al., 1993, McLennan et al., 1995). As a result of U-Pb fractionation, the

sedimentary and gneissic reservoirs evolve along separate trajectories in $^{207}\text{Pb}/^{204}\text{Pb}$ - $^{206}\text{Pb}/^{204}\text{Pb}$ space. By 1.93-1.97 Ga, the age of granitic magmatism in the TMZ, the sediment has developed a much more radiogenic Pb isotope composition than the gneiss. Tectonic burial during orogenesis results in the production and mixing of magmas derived from both sedimentary and gneissic sources. In this model, the range in Pb isotope compositions of the TMZ granitoids reflects the variable proportion of gneissic or sedimentary end member contributing to a specific granite sample. However, the slope of the data array also reflects the time elapsed since the two end members involved in the mixing process had a uniform Pb isotope composition.

Such a model is geologically reasonable in that the TMZ granitoids intrude through or near gneisses of the late Archean Churchill craton. Sediments derived in large part from the craton, the so-called Rutledge River Basin sediments, are also found scattered throughout the TMZ and as enclaves in some of the TMZ granites (Bostock and van Breeman, 1994). The time at which the detritus in these metasedimentary rocks was first produced by erosion of the cratonic gneisses is not known. However, the high $^{87}\text{Sr}/^{86}\text{Sr}$ values of the metasediments at 1.9-2.0 Ga (Baadsgaard and Godfrey, 1972) indicate a long residence time in a high Rb/Sr reservoir such as a sediment. Similarly, the chemical maturity of the sediments, which are mostly high Al pelites and quartzites, is consistent with a long sedimentary history and possibly several cycles of sedimentation. These observations suggest early separation of sedimentary detritus from Archean-age gneissic source rocks, and consequently early U-Pb fractionation between these two reservoirs. Partial melting of a source region consisting of both metasediments and gneisses at 1.97-1.93 Ga would have produced the range of Pb isotope compositions found in the TMZ granitoids.

Oxygen Isotopes

Fig. 13 shows comparative histograms of $\delta^{18}\text{O}$ values from the eastern and the western plutons, the metasediments and the TBC gneisses. The high $\delta^{18}\text{O}$ values of all the TMZ granites indicate extensive contribution to the magma from crustal protoliths formed or modified in a low-temperature environment. More specifically, the $\delta^{18}\text{O}$ values of the Slave granitoid samples overlap the values obtained for the metasediments and is consistent with other evidence presented above that the granites were derived from partial melting of these metasediments. The data for the Arch Lake granites are more difficult to interpret. These granites have high $\delta^{18}\text{O}$ values indicating a large sedimentary component in their source region but Pb isotope compositions that are unlike those of most of the metasediments that have been analyzed from the TMZ (Fig.11). One metasedimentary sample (TMZ -38B), however, has a distinctly unradiogenic Pb isotope composition broadly like the Arch Lake granites. It is possible that such a metasedimentary source rock, characterized by high $\delta^{18}\text{O}$ but unradiogenic Pb, was a major contributor to the Arch Lake magmas. The $\delta^{18}\text{O}$ values of the eastern plutons lie in between values obtained for the metasediments and TBC gneisses. This is consistent with the conclusion reached from Pb isotope data that these granites could be derived from a mixture of metasedimentary and gneissic sources. Importantly, none of the $\delta^{18}\text{O}$ values of the TMZ granites are close to mantle $\delta^{18}\text{O}$ values of +5 to +6‰ (Hoefs 1997), indicating little contribution to the granites from mantle sources.

Assimilation and Fractional Crystallization:

To test further the idea that a subduction-related mantle magma was involved in the generation of the eastern plutons, we considered simple assimilation-fractional crystallization (AFC) models calculated using the principles of Taylor (1980; 1986) and DePaolo (1981). The AFC process, which is proposed to be important in many subduction zone environments (James et. al., 1980; 1982; 1984; Hildreth & Moorbath 1986), generates mixing trajectories different from those produced by simple two component mixing or crystal fractionation (Fig. 14). For modeling, we chose a basaltic magma with a depleted mantle isotopic composition ($^{143}\text{Nd}/^{144}\text{Nd} = 0.510392$ @ 1.97Ga, $\delta^{18}\text{O} = 5.5\text{‰}$) and a Nd abundance typical for island-arc basalts (25 ppm, Hawkesworth et. al., 1979). Possible crustal assimilants include the TBC gneisses and the metasediments. The gneisses can be ruled out *a priori* because their $\delta^{18}\text{O}$ values are too low to produce the eastern plutons at any degree of assimilation. We therefore chose to model a TMZ metasediment as a potential assimilant ($^{143}\text{Nd}/^{144}\text{Nd} = 0.50985$ @ 1.97Ga, Nd = 30ppm, $\delta^{18}\text{O} = 12\text{‰}$). For the bulk distribution coefficient of Nd, we chose $D_{\text{Nd}} = 0.5$ as studies have shown that for various mafic magma and assimilant compositions, the fractionating phases have $D_{\text{Nd}} < 1$ (Nielsen, 1989). Our calculations indicate that varying D_{Nd} from 0.3 to 1 has a relatively minor effect on the position of the calculated curves. AFC trajectories were calculated and plotted (Fig. 14) using standard equations (Taylor, 1986). For the parameter R, which is the ratio of the mass of cumulates to assimilated crust, we chose a range of values between 1.5 and 5 (Taylor, 1986). R values of 1.5 indicate that the assimilated crust (metasediments) is very hot even before incorporation in the basalt. Cooler crust is modeled by R = 5 (Taylor, 1986). The AFC curves were drawn until near complete crystallization of the melt as indicated by the F values of 0.01,

where F is the mass of magma remaining as a fraction of original magma mass (Fig.14). It is evident from the plot that assimilation of existing TMZ basement gneiss or metasediment samples by a mantle-derived basaltic magma cannot account for the isotopic compositions of the eastern plutons.

In summary, the isotopic data presented in this study show no evidence of a significant mantle-derived component in either the early I-type or the later S-type magmas of the southern TMZ. Instead, the data indicate derivation of these magmas from metaigneous and metasedimentary crustal sources of late Archean age. These findings have important implications for the tectonic setting in which the TMZ magmas originated.

Comparison with Phanerozoic continental margin magmatism

To evaluate the link between magmatism and tectonics in the TMZ, we have compared our isotopic data for the TMZ granites with data from two Phanerozoic continental margin settings, the Central Volcanic Zone (CVZ) of southern Peru and northern Chile, and the precollisional Trans-Himalaya batholith of Tibet. We chose these areas because they represent well-documented examples of magmatism caused by subduction of oceanic crust underneath a continental margin. Both areas have, in fact, been suggested as possible Phanerozoic analogues for the early development of the Taltson-Thelon orogen (Hoffman, 1988; 1989; Ross et al.,1991; Windley 1992). If the analogy is appropriate then the early I-type TMZ granitoids, which are proposed to be related to subduction, should resemble magmatic rocks found in these areas.

In the CVZ, subduction of the oceanic Nazca plate beneath continental crust of the South American plate has given rise to volcanic and plutonic rocks with compositions ranging from basalt through rhyolite (James et al. 1971; 1981; 1982; 1984; Harmon et al. 1984). The tectonic environment of the CVZ differs from other parts of the Andes in that subduction has occurred under 60-70 km thick continental crust. This unusually large

thickness of continental crust has provided extensive opportunity for contamination of mantle-derived magmas by crustal material (James et al. 1981; 1982; Harmon et al. 1984). The Trans-Himalaya batholith, which extends for more than 2500 km along the northern side of the Indus-Tsangpo suture zone, formed in a broadly similar environment. It is the product of northward subduction of neo-Tethys oceanic crust beneath the continental margin of Asia (Searle et al. 1992; Windley, 1997). The batholith comprises predominantly plutonic rocks ranging from quartz diorite to granite in composition (Debon et al. 1986). There is an extensive set of oxygen and neodymium isotope data available for the CVZ (James et al. 1982; Harmon et al. 1984, Longstaffe et al. 1983) and a more limited set of oxygen isotope data for the Trans-Himalaya (Debon et al. 1986) which can be compared with our data from the southern TMZ.

Fig.15 shows a plot $^{143}\text{Nd}/^{144}\text{Nd}$ versus $\delta^{18}\text{O}$ for volcanic rocks from the CVZ. According to James et al. (1982), these rocks were produced by contamination of mantle-derived magmas by Precambrian age continental crust represented by the Charcani gneiss. Importantly, the samples from the CVZ plot in between the composition of depleted mantle and the likely crustal contaminant, reflecting a significant contribution to the magmas from both mantle and crustal sources. In contrast, the isotopic compositions of the early TMZ granitoids overlap those of TMZ basement rocks indicating direct derivation from crustal sources with little or no mantle contribution (Fig. 16).

A similar conclusion can be reached by comparing oxygen isotope data from the eastern TMZ plutons with that available from the CVZ and the Trans-Himalaya batholith (Fig. 17). It is evident that the TMZ granitoids are systematically higher in $\delta^{18}\text{O}$. Only one analyzed TMZ granitoid sample has $\delta^{18}\text{O}$ value lower than +8‰ whereas the majority of samples from the CVZ and the Trans-Himalaya have $\delta^{18}\text{O}$ values below +8‰. The lower $\delta^{18}\text{O}$ values associated with subduction-related magmatism reflects contribution to

these magmas from both mantle ($\delta^{18}\text{O} = +5\text{-}6\text{‰}$) and crustal (typically $\delta^{18}\text{O} >7.5\text{‰}$) sources. TMZ magmatism, on the other hand, can be explained by melting of exclusively crustal sources.

The comparison of isotopic data presented above shows that early TMZ magmatism was unlike that found at modern-day continental margins experiencing subduction of oceanic crust. More specifically, the TMZ granitoids lack the mantle isotopic signature that is apparent in continental margin magmas even in cases such as the CVZ where these magmas intruded through thick continental crust. The absence of a significant mantle contribution to TMZ magmatism is corroborated by other petrological and geochemical data. The early TMZ granitoids are dominated by granodiorites and granites unlike the quartz diorite-tonalite-granodiorite suite of plutonic rocks typical of continental margins (Pitcher, 1993). Similarly, felsic magmatism in the TMZ is not associated with significant amounts of basaltic magmatism whereas the latter is widespread at modern-day continental margins experiencing subduction. Geochemically, the TMZ granitoids are characterized by a paucity of samples with less than 63 wt. % SiO_2 . In contrast, granitoids formed at destructive plate margins during both Phanerozoic and Proterozoic times contain many samples with 55 to 65 wt. % SiO_2 (Hawkesworth et al., 1979; Harmon et al., 1984; Debon et al., 1986; Hildebrand et al., 1987; Crawford and Searle, 1992).

Collectively, these isotopic, petrological and geochemical data strongly suggest that TMZ magmatism did not occur at a destructive plate margin. This conclusion bears directly on the tectonic model that had been proposed for the TMZ. We believe that the existing model of subduction followed by collision at a continental margin is no longer tenable in light of the data acquired in this study. Below, we present an alternative model that better accounts for the nature of magmatic activity in the TMZ and discuss the

implications of this new model for the tectonic assembly of the western part of the North American craton.

Towards an alternate tectonic model

The basic premise of the previous tectonic model is that linear magmatic belts of a broadly calc-alkaline nature form only at plate margins. This, however, is not the case. For example, magmatism in the North American Cordillera during the Mesozoic occurred along two parallel belts, both of which extend discontinuously along strike for more than 3000 km from Mexico to Alaska. One belt is located along the continental margin and represented by subduction-related batholiths such as Peninsular Ranges, Sierra Nevada and Coast Range batholiths (Bateman et al., 1970; Silver et al., 1979; Roddick, 1983; Barker et al., 1984; Gromet and Silver, 1987; Barker and Arth., 1990) The second belt is located 400-800 km inland from the continental margin and represented by the Idaho, Fry Creek, White Creek and Cassiar batholiths, as well as numerous smaller plutons in British Columbia, Washington, Utah, Nevada and Arizona. Although magmatism in the two belts was broadly synchronous, there are clear geochemical and isotopic differences between the two suites of rocks. Unlike typical magmatic rocks of continental margins, the Cordilleran interior batholiths are dominated by felsic rocks (mostly >63 wt. % SiO₂) (Miller and Barton, 1990). Metaluminous, weakly peraluminous and strongly peraluminous granitoids are present in this suite but peraluminous rocks typically dominate (Miller and Barton, 1990). Many of the interior batholiths are characterized by a conspicuous absence of contemporaneous basaltic composition magmatism (Miller and Barton, 1990; Farmer, 1992; Driver et al., 1998). Isotopic data indicate a predominantly, if not an exclusively, crustal source region for these granitoids, consisting of both metaigneous and metasedimentary rocks (Farmer, 1992; Brandon and Lambert, 1994; Driver et al., 1997). All of the isotopic and geochemical features noted above are shared

by the southern TMZ granitoids. We suggest, therefore, that the Cordilleran interior granitoids provide a much better analogue for TMZ magmatism than do the granitoids of continental margins.

The tectonic setting in which Cordilleran interior magmatism occurred is still debated (e.g., Miller and Barton, 1990). However, there is a growing consensus that these granitoids are not directly related to subduction, but are the product of crustal thickening and associated intra-crustal melting in the hinterland of a convergent plate margin (Patino-Douce et al., 1990; Pitcher, 1993; Brandon and Lambert, 1994; Driver et al., 1998). A possible example of this process occurring in the present day is the Tien Shan area of central Asia. The Tien Shan is a late Cenozoic mountain belt that has formed 700-1000 km inland from the Indus-Tsangpo suture zone (Burg et al. 1997, Neil and Houseman, 1997; Windley, 1997). Although distant from the plate margin, compressional tectonism and crustal thickening in the Tien Shan is the product of far-field stresses associated with India-Asia collision (Windley, 1997; Neil and Houseman, 1997). Windley (1997) suggests that the lower crust of the Tien Shan and adjacent areas may presently be undergoing high-grade metamorphism and partial melting as a result of this tectonism. This is supported by seismic evidence which indicates that there is a northward increase in melt fraction within the crust of the Tibetan plateau (Hirn et al. 1997).

We propose that the TMZ is an early Proterozoic example of such an intra-continental orogenic belt where crustal thickening and associated magmatism occur inboard from a convergent plate margin. Importantly, in our model, TMZ magmatism is not triggered by the influx of subduction-related mafic magma into the crust as is the case at convergent plate margins. Rather, it is fundamentally an intra-crustal process, occurring in response to crustal thickening in the continental interior. During the thickening event, melting proceeds generally upward in the crust, involving first a

predominantly metaigneous lower crust followed by a largely metasedimentary middle crust. This gives rise to the early I-type followed by the later S-type character of magmatism in the TMZ.

Implications for the assembly of the North American craton

The data reported in this study are for samples from the southern part of the TMZ. As such, the conclusions drawn above are strictly applicable only to that segment of the TMZ. However, on the basis of available geochemical and isotopic data (Theriault, 1992), we propose that the granitoids of the northern TMZ had a very similar origin. In particular, except for a slightly more juvenile Nd isotope composition, the early Deskenatlata suite granitoids of the northern TMZ, which had been ascribed to subduction, share virtually all the geochemical and petrological features of the eastern plutons of the southern TMZ. We suggest, therefore, that our tectonic model is applicable to the Deskenatlata granitoids and to the entire exposed length of the TMZ. Our model may also be applicable to the northward extension of the TMZ, the Thelon orogen, although the geochemical and isotopic data necessary to evaluate this hypothesis in detail are not yet available for that area. At the very least, we believe the findings of our study warrant a thorough re-evaluation of the tectonic model that has been proposed for the Thelon (Hoffman, 1987; 1988).

If our conclusions can, in fact, be extrapolated, there are far reaching implications for the tectonic assembly of the western part of the North American craton. Our model implies that the various crustal blocks flanking the Taltson-Thelon orogenic belt were not brought together by consumption of oceanic crust at 1.9-2.0 Ga (e.g., Hoffman, 1988) but became a coherent entity before that time (Fig. 1). One possibility is that these blocks originally formed together. That is, the Churchill craton, the Buffalo Head Terrane, and possibly the Slave craton formed as a single cratonic block in the Archean. Indeed,

Theriault (1994) and Bostock and van Breeman (1994) note many isotopic similarities between the crust of the Churchill craton and the Buffalo Head Terrane and suggest that the two represent variably reworked fragments of the same Archean crustal block. In contrast, sharp gravity and magnetic gradients across the Slave-Churchill boundary (Gibb and Thomas, 1977; Hoffman, 1987), suggest that these are two distinct crustal blocks that were assembled after formation. A possibility consistent with this observation, and with our tectonic model, is that two or all three blocks formed separately but were sutured together prior to 2.0 Ga. In this regard, it is interesting to note that 2.3-2.4 Ga granitoids and granitic orthogneisses have been recognized along the entire length of the TMZ (Bostock and Loveridge, 1988; van Breeman et al., 1991; and McNichol et al., 1994). Granitoids of this age may also be present in the Thelon orogen (van Breeman et al., 1987). Available geochemical data from the southern TMZ (Goff et al., 1986) suggest more arc affinities for these older granitoids than for any of the 2.0-1.9 Ga granitoids discussed in this paper. Thus, it is possible that these earliest TMZ granitoids represent the vestiges of a 2.3-2.4 Ga continental margin arc that was present during assembly of the various blocks (cf. Bostock and van Breeman, 1994). The point that must be emphasized here is that the process of crustal assembly took place before 2.0 Ga, and was not associated with the formation of the dominant 2.0-1.9 Ga magmatic rocks of the TMZ.

A question that remains is the location of the plate margin during TMZ magmatism. Although its precise location cannot be constrained from the available data, we can make reasonable speculations. The two primary criteria in locating the plate margin are the age and geochemical characteristics of magmatism. Magmatism associated with this plate margin has to be concurrent with that occurring in the TMZ. Unlike TMZ magmatism, however, this plate margin magmatism should have arc-like geochemical characteristics. Major early Proterozoic magmatic belts are, in fact, present both to the

east and west of TMZ (Fig.1) These include the Trans-Hudson, Great Bear, and Fort Simpson belts (Hildebrand et al., 1987; Hoffman, 1988 and references therein). Available U-Pb age data, however, indicate that magmatism in these belts occurred after 1.9Ga (Bowring, 1985; Hildebrand et al., 1987) and thus is too young to be associated with the formation of the TMZ. In contrast, some magmatic rocks in the poorly exposed Hottah terrane predate 1.94 Ga (Bowring and Grotzinger, 1992). Similarly, magmatic rocks in the western part of the subsurface Buffalo Head terrane and Ksituan magmatic belt have ages near 2.0 Ga (Ross et al., 1991, Villeneuve et al., 1993). These may represent the plate margin associated with TMZ magmatism although more geochemical data are needed to evaluate this idea.

CONCLUSIONS

Our main objective in this paper was to study the geochemical and isotopic character of granitoids from the southern TMZ with a view to understanding the tectonic environment in which these granites formed. Our data indicate that the strongly peraluminous granites of the TMZ were derived from partial melting of metasedimentary rocks, similar to those occurring as enclaves in some of these granites. This result is consistent with the findings of earlier studies and with the idea that these S-type granites formed in a collisional tectonic setting (Hoffman, 1988; Theriault, 1992; Chacko et al., 1995). Our results do not support the currently accepted hypothesis for the origin of early I-type granitoids in the TMZ. Isotopic and geochemical data suggest that these granitoids were derived from a mixed metagneous and metasedimentary crustal source of late Archean age. Importantly, the data show little evidence for a mantle contribution to these granitoids. This is distinctly unlike Phanerozoic examples of continental margin magmatism where a significant mantle input is apparent. Therefore, we argue that the existing Andean-type model for early TMZ magmatism is not viable. Instead, we propose

that the I-type and S-type granitoids of the TMZ are akin to those found in the hinterland of convergent plate margins. Our tectonic model for the TMZ is analogous to the tectonic setting of the Cordilleran interior of western North America and the Tien Shan area of central Asia where crustal thickening and associated magmatism occur inboard from a convergent plate margin. The broader implication of this model is that the Taltson-Thelon orogenic belt does not mark the location of the plate boundary of the North American craton at 1.9-2.0 Ga. Rather, the crustal blocks flanking the belt must have been assembled before 2.0 Ga. The precise location of the plate margin associated with TMZ magmatism cannot be rigorously constrained with the available data. We speculate, however, that the 1.94-2.0 Ga magmatic rocks in the Hottah terrane, the western Buffalo Head terrane and the Ksituan belt may represent the plate margin during TMZ magmatism.

Table 1. Major and trace element abundances of samples from TMZ.

Sample Type	TMZ1 1	TMZ2 1	TMZ5 1	TMZ6 1	TMZ8 1	TMZ9 2	TMZ10 2	TMZ11 2	TMZ13 2
<i>Major element (wt %)</i>									
SiO ₂	73.85	73.2	62.46	65.56	65.57	71.21	71.91	73.02	72.87
Al ₂ O ₃	14.67	14.96	17.13	16.1	15.53	15.58	14.67	14.68	14.76
TiO ₂	0.241	0.168	0.77	0.57	0.513	0.319	0.327	0.247	0.204
FeO ^T	1.95	1.19	5.56	4.47	4.31	1.53	2.1	1.33	1.4
MnO	0.034	0.014	0.07	0.07	0.08	0.014	0.019	0.012	0.017
CaO	1.72	1.48	4.39	4.09	3.7	1.38	1.49	0.66	1.2
MgO	0.96	0.67	3.36	2.67	3.15	0.74	0.91	0.61	0.51
K ₂ O	1.81	4.88	2.94	2.82	3.83	5.3	4.98	6.83	5.54
Na ₂ O	4.65	3.37	2.99	3.30	3.17	3.84	3.47	2.48	3.4
P ₂ O ₅	0.1	0.069	0.337	0.34	0.137	0.086	0.132	0.121	0.095
<i>Trace element (ppm)</i>									
Ba	416	1350	602	1054	1237	1384	1131	672	822
Rb	70.9	126.2	144.8	141.5	134.9	138.4	164.3	234.8	168.3
Cs	1.64	2.58	3.05	3.47	8.49	0.24	0.21	0.69	0.49
Sr*	266	269	651	563	343	215	237	118	181
Pb	26.25	51.22	17.45	19.16	18.02	33.84	36.9	36.43	46.24
Th	17.17	14.38	15.12	13.63	10.58	21.53	18.62	27.69	26.27
U	7.48	4.06	2.72	2.66	3.39	1.95	1.17	4.36	2.76
Zr*	112	90	205	185	130	215	157	135	126
Nb	10.94	7.77	11.06	11.08	9.09	9.62	7.96	12.52	7.55
Hf	3.17	2.59	5.45	4.89	3.88	6.15	4.39	3.96	3.78
Ta	2.61	2.85	1.02	1.45	1.17	2.08	0.45	2.4	0.54
Y	15.43	13.06	25.73	25.44	14.62	8.53	8.94	9.44	7.9
La	40.00	35.71	76.33	72.45	32.65	67.96	50.86	53.67	50.17
Ce	73.78	66.6	144.51	135.74	58.81	116.45	86.9	106.72	92.52
Pr	7.55	6.96	15.66	14.7	6.1	11.36	8.44	11.13	9.53
Nd	26.96	25.05	60.2	57.02	23.18	38.2	29.07	39.18	34
Sm	5.07	4.85	11.08	10.74	4.49	6.17	5.48	6.91	6.39
Eu	1.07	1.19	2.34	2.13	1.04	1.09	0.97	0.79	0.96
Gd	3.58	3.89	7.32	7.02	3.33	3.67	3.54	3.58	3.67
Tb	0.54	0.59	1.01	0.94	0.48	0.43	0.45	0.45	0.41
Dy	2.86	2.96	5.25	5.08	2.76	1.95	2.06	2.08	1.86
Ho	0.54	0.46	0.96	0.93	0.53	0.3	0.33	0.33	0.3
Er	1.35	0.85	2.31	2.31	1.41	0.71	0.75	0.79	0.7
Tm	0.2	0.1	0.3	0.32	0.21	0.1	0.11	0.1	0.1
Yb	1.22	0.48	1.62	1.96	1.32	0.64	0.63	0.64	0.65
Lu*	0.18	0.07	0.24	0.3	0.22	0.11	0.1	0.11	0.11
Sc*	7	4	16	11	14	3	2	1	7
V*	35	18	126	100	88	26	28	3	23
Cr*	29	1	40	54	85	9	16	1	9
Ni*	15	5	13	23	9	7	9	7	7
Cu*	9	9	8	17	17	12	25	6	18
Zn*	31	20	61	70	68	41	52	39	33
Ga*	16	16	22	22	22	24	24	21	21

Table 1. continued.

Sample Type	TMZ16 2	TMZ17 2	TMZ22 3	TMZ23 3	TMZ27 3	TMZ30 3	TMZ31A 4	TMZ33 4	TMZ35 4
<i>Major element (wt %)</i>									
SiO ₂	73.35	72.71	70.43	66.44	66.84	68.92	73.33	75.14	72.45
Al ₂ O ₃	14.2	14.7	14.37	14.89	16.33	15.48	15.31	14.67	15.45
TiO ₂	0.249	0.28	0.389	0.501	0.492	0.661	0.11	0.075	0.103
FeO ^T	1.31	1.27	2.69	3.47	3.6	3.71	0.93	0.51	1.46
MnO	0.011	0.015	0.058	0.057	0.07	0.039	0.024	0.002	0.016
CaO	0.71	0.96	2.05	2.79	2.8	2.6	0.92	0.52	0.66
MgO	0.84	0.47	2.32	2.6	1.85	1.47	0.29	0.27	0.32
K ₂ O	6.53	6.22	4.38	6.18	4.43	3.75	4.86	5.53	5.56
Na ₂ O	2.68	3.25	3.14	2.81	3.4	3.19	4.08	3.15	3.83
P ₂ O ₅	0.131	0.128	0.177	0.266	0.19	0.19	0.133	0.143	0.163
<i>Trace element (ppm)</i>									
Ba	727	1001	1285	2678	1169	1243	355	169	304
Rb	221.2	175	151.5	203.6	164.3	119.5	296.6	209.7	256.8
Cs	0.61	0.44	6.19	4.11	2.93	1.04	7.16	0.33	0.47
Sr*	134	155	341	583	383	238	93	62	99
Pb	36.76	34.66	27.91	43.06	26.13	20.03	37.82	48.44	59.93
Th	34.53	37.34	22.7	25.21	17.19	17.24	5.03	1.78	3.8
U	6.33	3.31	6.03	5.59	1.86	1.5	4.2	1.72	2.12
Zr*	159	169	141	174	174	241	62	38	56
Nb	15.99	11.06	12.35	12.97	13.06	11.98	9.92	3.54	6.66
Hf	4.79	4.92	4.02	4.71	4.69	6.18	2.04	1.31	1.86
Ta	3.44	2.91	2.42	2.89	1.93	2.18	3.46	1.34	1.99
Y	13.75	11.99	14.57	17.19	20.78	16.66	9.39	5.53	11.06
La	55.7	60.42	41.88	57.38	52.36	78.29	15.21	7.38	12.64
Ce	111.74	121.75	75.19	101.95	96.76	139.24	27.27	14.26	24.76
Pr	11.62	13.12	7.57	10.6	10.31	14.05	2.71	1.52	2.62
Nd	41.15	46.12	27.16	39.44	38.32	50.38	9.37	5.72	9.49
Sm	7.26	7.63	5.15	7.26	7.55	8.19	1.91	1.54	2.41
Eu	0.65	0.82	1.11	1.59	1.59	1.65	0.42	0.37	0.55
Gd	4.16	4.15	3.56	5.1	5.37	5.45	1.62	1.27	2.53
Tb	0.58	0.52	0.5	0.66	0.78	0.69	0.29	0.21	0.47
Dy	2.89	2.46	2.76	3.51	4.25	3.58	1.67	1.16	2.46
Ho	0.49	0.43	0.51	0.64	0.77	0.64	0.31	0.2	0.39
Er	1.14	0.98	1.35	1.55	1.89	1.52	0.87	0.46	0.94
Tm	0.15	0.12	0.2	0.23	0.25	0.2	0.14	0.06	0.14
Yb	0.86	0.7	1.26	1.46	1.39	1.19	0.85	0.4	0.82
Lu	0.13	0.11	0.2	0.24	0.2	0.19	0.13	0.06	0.12
Sc*	1	3	8	6	11	11	2	1	4
V*	11	25	52	67	66	67	1	5	0
Cr*	0	1	62	89	17	8	1	0	0
Ni*	3	2	15	26	19	7	8	7	10
Cu*	4	8	3	8	10	11	13	11	10
Zn*	37	40	48	54	61	55	41	20	37
Ga*	20	21	19	20	21	19	22	24	22

Table 1. continued

Sample	TMZ36	TMZ38A	TMZ39A	TMZ40	TMZ42	TMZ37	TMZ38B	628-4	616-1
Type	5	4	4	4	2	5	5	6	6
<i>Major element (wt %)</i>									
SiO ₂	62.87	72.97	68.37	71.43	73.79	62.62	77.8	62.73	58.43
Al ₂ O ₃	21.47	15.11	15.71	14.32	14.77	18.05	10.94	16.23	13.8
TiO ₂	0.889	0.072	0.725	0.327	0.131	0.884	0.501	0.739	0.728
FeO ^T	7.32	0.74	3.73	2.58	0.86	6.87	2.87	6.00	7.33
MnO	0.057	0.011	0.044	0.055	0.01	0.085	0.042	0.119	0.121
CaO	0.24	1.01	2.81	2.46	1.29	1.17	0.93	4.49	5.14
MgO	2.41	0.57	1.49	1.4	0.3	2.78	1.08	3.05	5.95
K ₂ O	3.98	6.36	3.63	4.07	4.63	5.48	3.81	2.8	6.18
Na ₂ O	0.73	3.06	3.28	3.24	4.19	1.98	1.98	3.62	1.69
P ₂ O ₅	0.031	0.95	0.206	0.106	0.043	0.083	0.055	0.218	0.63
<i>Trace element (ppm)</i>									
Ba	903	1041	1293	859	1449	1224	750	735	4442
Rb	135.7	202.3	132.7	165.1	127.1	245.4	128	103.2	282.3
Cs	2.34	1.31	1.33	0.89	0.45	2.91	1.36	0.74	35.82
Sr*	84	215	238	264	301	160	123	466	779
Pb	26.44	43.91	23.05	34.29	35.29	27.95	21.37	13.45	28.5
Th	3.33	2.76	22.54	16.6	6.26	12.56	12.67	4.48	13.1
U	0.48	1.69	1.86	2.47	1.04	1.93	1.6	0.63	3.55
Zr*	135	50	300	118	80	151	192	197	165
Nb	14.06	2.25	13.61	8.81	4.52	18.74	9.95	13.05	8.96
Hf	3.93	1.36	8.27	3.04	2.26	4.59	5.77	4.42	4.06
Ta	2.46	1.4	1.88	1.42	1.36	2.43	2.83	0.54	0.58
Y	11.64	10.22	19.9	11.62	2.16	28.44	18.98	20.07	22.71
La	16.71	15.4	93.79	30.76	17.67	35.96	32.17	43.22	41.12
Ce	27.51	26.52	166.18	53.98	27.66	68.24	61.42	82.35	77.57
Pr	2.73	2.59	16.76	5.43	2.54	7.18	6.36	9.2	8.96
Nd	9.75	8.97	59.32	19.6	8.61	27.34	23.62	36.45	36.81
Sm	2.34	1.75	9.96	3.72	1.56	5.68	4.79	7.46	8.00
Eu	1.25	1.25	1.68	0.88	0.52	1.41	1	1.58	2.03
Gd	2.5	1.52	6.67	2.8	1.14	5.09	3.87	5.2	6.01
Tb	0.41	0.24	0.84	0.4	0.13	0.86	0.63	0.77	0.86
Dy	2.52	1.58	4.33	2.2	0.53	5.3	3.45	4.09	4.59
Ho	0.54	0.36	0.77	0.42	0.08	1.06	0.7	0.77	0.87
Er	1.49	1.09	1.83	1.11	0.16	2.8	1.91	1.93	2.23
Tm	0.24	0.18	0.24	0.15	0.02	0.4	0.3	0.27	0.33
Yb	1.54	1.11	1.4	0.96	0.13	2.56	1.77	1.63	1.98
Lu	0.26	0.18	0.23	0.16	0.02	0.4	0.29	0.25	0.34
Sc*	13	2	11	9	4	17	10	17	22
V*	180	0	61	44	3	122	60	100	173
Cr*	181	2	9	44	0	94	48	102	309
Ni*	51	12	10	14	11	47	22	29	27
Cu*	83	50	3	4	7	28	6	13	25
Zn*	146	6	54	46	24	74	29	86	71
Ga*	27	19	20	18	19	25	14	23	16

Table 1. continued

Sample Type	628-6 6	104-3 6	616-2 6	232759 6	233588 6	TMZ 20 6
<i>Major element (wt %)</i>						
SiO ₂	77.89	67.00	73.15	64.44	71.18	71.63
Al ₂ O ₃	12.92	16.44	14.76	16.88	15.01	14.12
TiO ₂	0.038	0.626	0.151	0.72	0.349	0.395
FeO ^T	0.92	3.2	1.21	4.95	2.86	2.46
MnO	0.012	0.044	0.032	0.085	0.041	0.039
CaO	0.26	1.07	0.76	3.54	2.53	1.43
MgO	0.35	1.00	0.58	2.55	1.33	0.91
K ₂ O	2.02	7.13	5.1	3.14	2.38	5.58
Na ₂ O	5.56	3.37	4.21	3.34	4.23	3.32
P ₂ O ₅	0.03	0.121	0.058	0.361	0.083	0.103
<i>Trace element (ppm)</i>						
Ba	118	2659	1073	992	1311	1043
Rb	81.1	174.6	222	167.1	108.1	147.6
Cs	0.81	0.51	12.56	3.39	2.45	0.36
Sr*	74	235	306	518	329	255
Pb	23.59	18.15	44.9	22.31	22.67	18.13
Th	17.78	11.36	21.94	17.09	10.51	18.47
U	6.8	0.85	4.68	4.67	1.25	0.94
Zr*	73	563	104	243	175	214
Nb	41.3	25.95	11.24	8.98	5.83	10.68
Hf	4.19	10.76	2.99	5.21	3.31	5.85
Ta	1.18	0.99	1.35	0.79	1.04	3.57
Y	29.5	24.25	9.18	20.52	8.69	12.1
La	6.64	116.3	28.42	100.4	42.16	58.24
Ce	13.39	213.1	48.82	187.9	70.12	109.85
Pr	1.61	22.86	4.76	20.18	6.92	11.4
Nd	6.85	85.18	16.66	74.62	24.24	40.22
Sm	3.12	13.21	3.1	12.6	3.89	6.38
Eu	0.39	2.69	0.68	2.46	0.85	1.35
Gd	4.05	8.06	2.15	7.39	2.91	4.05
Tb	0.92	1.07	0.31	0.94	0.36	0.51
Dy	6.4	5.53	1.74	4.57	1.86	2.51
Ho	1.38	0.97	0.3	0.77	0.32	0.43
Er	4.16	2.2	0.79	1.75	0.7	0.94
Tm	0.69	0.31	0.13	0.24	0.1	0.12
Yb	4.65	1.72	0.79	1.33	0.59	0.73
Lu	0.71	0.28	0.13	0.21	0.1	0.12
Sc*	4	10	0	15	6	0
V*	8	16	18	102	32	30
Cr*	19	19	10	33	29	0
Ni*	13	7	10	17	24	0
Cu*	17	8	6	12	18	43
Zn*	7	26	32	91	49	0
Ga*	18	21	21	24	20	15

Major element analyses performed by XRF and normalised to 100% (volatile free). Trace elements except where indicated, analysed by ICPMS. * Trace elements analysed by XRF. Rock type: 1- Wylie Lake granite; 2 - Arch Lake granite; 3 - Colin Lake granite; 4 - Slave granite; 5 - TMZ metasediments; 6 - TBC gneisses.

Table 2. Sm-Nd isotope analyses of samples from TMZ.

Sample	Sm (ppm)	Nd (ppm)	$^{147}\text{Sm}/^{144}\text{Nd}$	$^{143}\text{Nd}/^{144}\text{Nd}^a$	$\epsilon\text{Nd}_{\text{DM}}^b$	T_{DM}^c
Arch Lake Granitoids						
TMZ 9	4.98	34.86	0.0864	0.510820 (10)	-8.2	2.8
TMZ 10	5.07	30.38	0.1009	0.510971 (11)	-8.8	2.9
TMZ 11	6.88	45.19	0.0921	0.510948 (10)	-7.1	2.8
TMZ 13	4.12	25.06	0.0955	0.511076 (12)	-6.4	2.8
TMZ 16	7.07	45.54	0.0939	0.510980 (14)	-6.9	2.8
TMZ 16(rpt)	7.05	45.79	0.0931	0.510955 (17)	-7.2	2.8
TMZ 17	7.62	52.24	0.0882	0.510871 (9)	-7.6	2.8
JG37-1*	6.37	41.83	0.0920	0.510969 (8)	-6.6	2.7
JG37-5*	9.34	64.42	0.0876	0.510906 (8)	-6.8	2.7
JG523-6*	6.46	40.29	0.0969	0.511071 (8)	-5.9	2.7
JG36-1*	4.69	32.53	0.0871	0.510888 (6)	-7.0	2.7
JG52-3*	5.37	34.84	0.0930	0.510970 (4)	-6.9	2.7
JG233-4*	2.58	20.19	0.0772	0.510855 (13)	-5.2	2.6
TMZ 42	1.53	9.33	0.0993	0.510900 (10)	-9.8	3.0
Slave Granitoids						
TMZ 31A	1.98	10.56	0.1133	0.511315 (9)	-5.2	2.8
TMZ 31A(rpt)	1.92	10.25	0.1133	0.511346 (18)	-4.5	2.7
TMZ 33	1.50	6.32	0.1440	0.511682 (15)	-5.6	3.2
TMZ 35	2.57	11.60	0.1337	0.511586 (9)	-4.9	3.0
JG39-2*	5.19	28.40	0.1104	0.511345 (5)	-3.8	2.7
JG9-1*	2.64	10.11	0.1576	0.511848 (7)	-5.7	3.5
JG28-7*	1.17	7.17	0.0991	0.510944 (9)	-8.9	2.9
JG68-3B*	0.49	3.18	0.0930	0.511148 (21)	-3.4	2.5
JG248-1*	2.71	12.56	0.1300	0.511589 (22)	-4.0	2.8
JG36-3*	5.35	29.87	0.1083	0.511259 (10)	-5.0	2.7
JG8-4*	1.79	7.86	0.1375	0.511687 (18)	-3.9	2.9
TMZ 38A	1.49	8.68	0.1034	0.511141 (8)	-6.1	2.8
TMZ 39A	8.26	54.96	0.0910	0.510991 (14)	-6.0	2.7
TMZ 40	4.56	24.06	0.1145	0.511277 (8)	-6.2	2.9
JG86-4*	7.17	47.53	0.0911	0.511087 (13)	-4.1	2.6

Sample	Sm (ppm)	Nd (ppm)	$^{147}\text{Sm}/^{144}\text{Nd}$	$^{143}\text{Nd}/^{144}\text{Nd}^a$	$\epsilon\text{Nd}_{(t)}^b$	T_{DM}^c
Slave Granitoids						
JG34-5*	6.26	32.07	0.1179	0.511291 (11)	-6.8	2.9
JG92-4*	2.38	15.39	0.0933	0.510950 (11)	-7.3	2.8
Wylie Lake Granitoids						
TMZ 1	4.98	29.89	0.1008	0.511135 (18)	-5.2	2.7
TMZ 2	3.82	22.18	0.1042	0.511205 (8)	-4.7	2.7
TMZ 6	10.03	57.43	0.1058	0.511293 (14)	-3.4	2.6
TMZ 8	4.92	27.63	0.1076	0.511181 (13)	-6.0	2.8
Colin Lake Granitoids						
TMZ 22	4.97	29.52	0.1017	0.511112 (15)	-5.8	2.8
TMZ 23	7.22	42.90	0.1017	0.511098 (13)	-6.0	2.8
TMZ 27	7.40	42.73	0.1047	0.511249 (11)	-3.9	2.7
TMZ 30	8.96	62.11	0.0873	0.510984 (14)	-4.6	2.6
Basement Gneisses						
TMZ 36A	2.55	12.18	0.1267	0.511475 (12)	-5.4	2.9
TMZ 37	5.18	27.86	0.1123	0.511307 (9)	-5.1	2.8
TMZ 20	5.92	40.62	0.0882	0.510840 (8)	-7.8	2.8
C233588	2.74	16.83	0.0985	0.510450 (8)	-17.9	3.6
C232759	12.76	83.47	0.0922	0.511127 (8)	-3.1	2.5
104-3	12.75	91.37	0.0843	0.510778 (6)	-7.9	2.8
JG93-1*	6.29	35.23	0.1079	0.511263 (5)	-4.4	2.7
JG98-2*	6.56	35.91	0.1103	0.511269 (6)	-4.9	2.8
JG104-1*	27.99	190.57	0.0887	0.510828 (3)	-8.0	2.8
JG104-2*	10.08	75.93	0.0802	0.510625 (5)	-9.8	2.9
JG105-11*	16.64	113.3	0.0887	0.510839 (4)	-7.8	2.8

a Normalized to $^{146}\text{Nd}/^{144}\text{Nd} = 0.7219$. Numbers in parentheses indicate 2σ uncertainties,

b ϵNd calculated at 1.93 Ga for Slave Lake and Arch Lake granitoids; 1.96 Ga for Wylie Lake granitoids; 1.97 Ga for Colin granitoids; and 1.97 Ga for Basement gneisses.

c T_{DM} calculated using the mantle evolution model of Goldstein et al. (1984). Present day CHUR parameters are $^{147}\text{Sm}/^{144}\text{Nd} = 0.1967$, $^{143}\text{Nd}/^{144}\text{Nd} = 0.512638$. $\lambda_{^{147}\text{Sm}} = 6.54 \times 10^{-12} \text{ a}^{-1}$

Sm-Nd analyses of samples denoted with an asterisk are from Dr. H. Baadsgaard (previously unpublished data).

Table 3. Lead isotopic composition of K-feldpars and whole rocks from TMZ.

Sample	$^{206}\text{Pb}/^{204}\text{Pb}$	$^{207}\text{Pb}/^{204}\text{Pb}$	$^{208}\text{Pb}/^{204}\text{Pb}$
Wylie Lake granitoids			
TMZ 1 Kfs	16.518	15.473	35.918
TMZ 2 "	15.606	15.305	35.188
TMZ 6 "	15.761	15.346	35.262
TMZ 8 "	15.645	15.338	35.371
TMZ 8L1	22.085	16.053	38.690
Arch Lake granitoids			
TMZ 9 Kfs	15.238	15.170	35.031
TMZ 9L1	17.574	15.453	43.135
TMZ 9L4	15.319	15.169	35.000
TMZ 10 Kfs	15.372	15.240	35.094
TMZ 10L1	16.664	15.381	40.070
TMZ 13 Kfs	15.284	15.191	35.014
TMZ 16 Kfs	15.431	15.202	35.325
TMZ 16 (rpt)	15.435	15.192	35.276
TMZ 42 Kfs	15.075	15.117	34.902
TMZ 42L1	18.410	15.503	38.129
TMZ 42L4	15.283	15.144	34.924
Slave granitoids			
TMZ 31 Kfs	16.117	15.410	35.248
TMZ 31L1	27.022	16.460	38.123
TMZ 31L4	16.849	15.467	35.349
TMZ 33 Kfs	15.769	15.346	35.110
TMZ 35 "	15.817	15.366	35.180
TMZ 39A "	15.820	15.373	35.350
TMZ 39A(rpt)	15.787	15.380	35.377
TMZ 40	15.771	15.380	35.303
Wylie Lake granitoids			
TMZ 1 Kfs	16.518	15.473	35.918
TMZ 2 "	15.606	15.305	35.188
TMZ 6 "	15.761	15.346	35.262
TMZ 8 "	15.645	15.338	35.371
TMZ 8L1	22.085	16.053	38.690
Colin Lake granitoids			
TMZ 22 Kfs	15.580	15.293	35.224
TMZ 23 "	15.485	15.266	35.232
TMZ 23L1	19.736	15.770	41.040
TMZ 23L4	15.735	15.287	35.340
TMZ 27 Kfs	15.536	15.324	35.330
TMZ 30 "	15.798	15.382	35.404
TMZ 40	15.771	15.380	35.303
Metasediments			
TMZ 36A Kfs	15.616	15.332	35.136
TMZ 37 Kfs	15.671	15.323	35.175
TMZ 38B "	15.222	15.064	35.060
Basement Gneisses			
616-1 Kfs	15.085	15.161	34.940
104-3 Kfs	14.713	15.024	34.840

L1 = leach 1 (24 hrs in 2N HCl), L4= leach 4 (24 hrs in 16N HNO₃ + 1 drop 48% HF);
Kfs =K-feldspar, WR = whole rock analyses.

Table 4. Oxygen isotope composition of samples from TMZ.

Sample	$\delta^{18}\text{O}$ (‰)	Sample	$\delta^{18}\text{O}$ (‰)
WYLIE LAKE:		SLAVE:	
TMZ 1	10.8	TMZ 31A	10.7
TMZ 2	9.9	TMZ 33	11.8
TMZ 2 Quartz	10.3	TMZ 35	11.3
TMZ 3	9.7	TMZ 39A	9.6
TMZ 4	10.5	TMZ 38A	11.6
TMZ 5	8.1	TMZ 40	10.1
TMZ 6	8.6	METASEDIMENTS	
TMZ 6 Quartz	11.3	TMZ 24	9.7
TMZ 7	9.6	TMZ 36A	10.8
TMZ 8	8.7	TMZ 37	9.3
COLIN LAKE		TMZ 37 Quartz	10.9
TMZ 21	7.8	TMZ 38B	10.7
TMZ 22	8.6	PR 2	9.9
TMZ 23	9.6	PR 4	9.4
TMZ 25	9.2	PR 10	9.5
TMZ 27	8.9	PR 12	9.8
TMZ 28	9.1	BASEMENT GNEISSES	
TMZ 29	9.4	C232759	8.8
TMZ 30	9.6	C233588	8.3
ARCH LAKE		628-4	7.3
TMZ 11	10.2	104-3	7.9
TMZ 13	9.7	TMZ 20	8.2
TMZ 16	10.2		
TMZ 17	10.9		
TMZ 9	10.8		
TMZ 10	10.6		

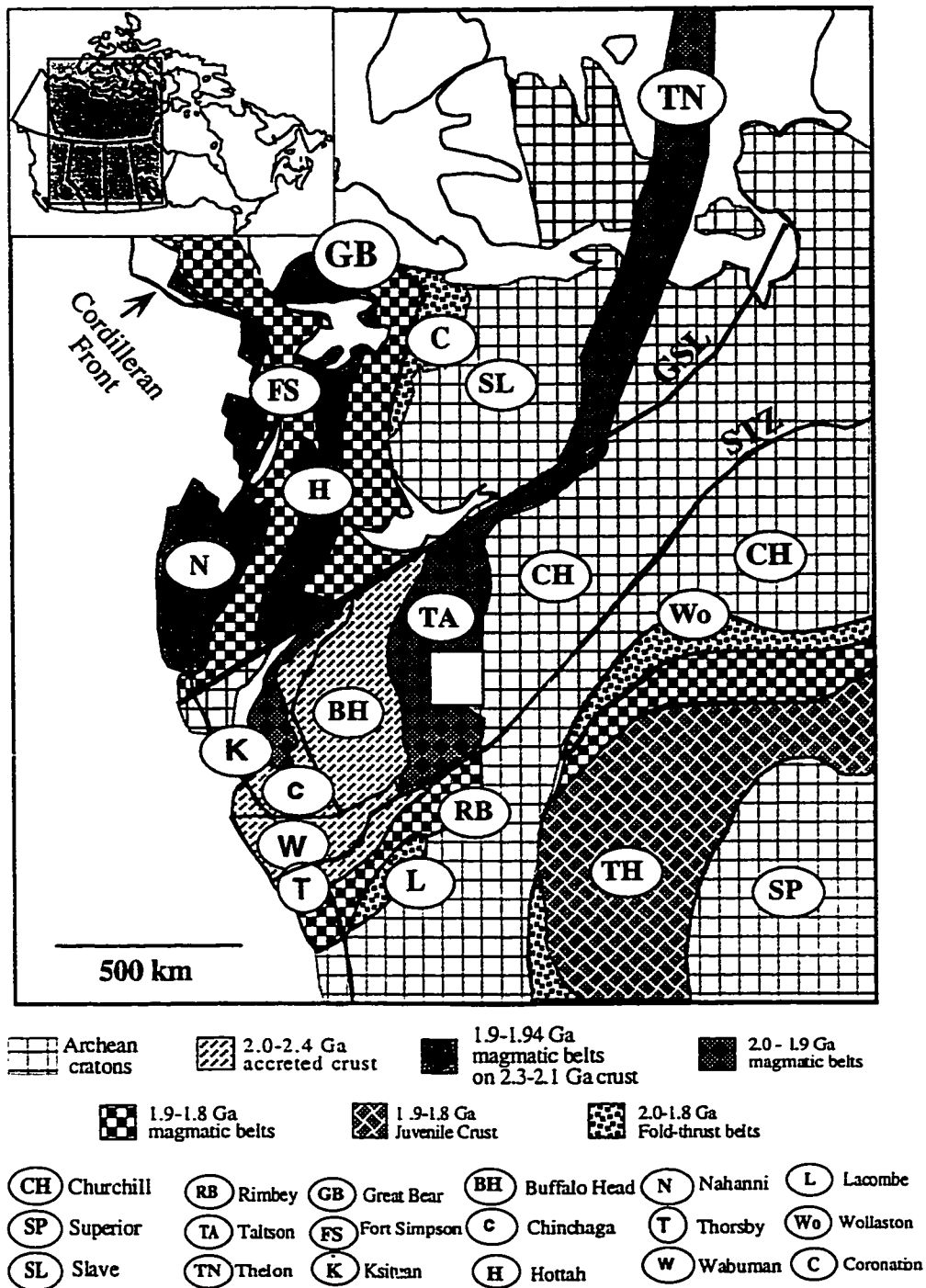


Fig 1. Generalized map showing tectonic elements of the Western Canadian Shield including the Taltson Magmatic Zone. Map is modified after Hoffman (1989) and McDonough et al.(1994). GSL and STZ denote Great Slave Lake Shear Zone and Snowbird Tectonic Zone, respectively. The outlined box indicates the present study area.

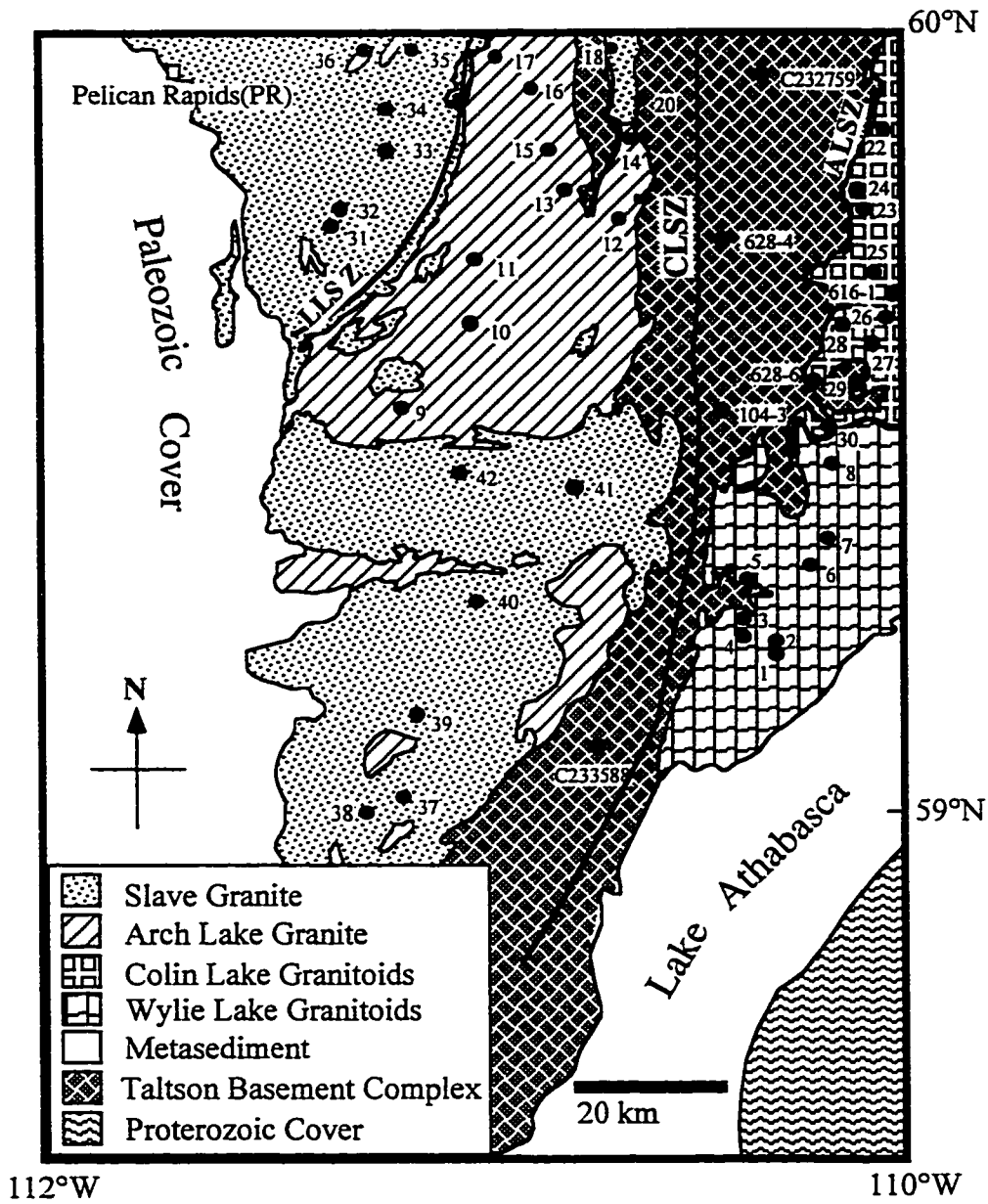


Fig 2. Generalized geological map of southern Taltson Magmatic Zone, NE Alberta showing sample locations of the present study. Numbers beside each sample location corresponds to sample numbers in Table 1. ALSZ= Andrew Lake shear zone, CSLZ= Charles Lake shear zone, LLSZ=Leland Lake shear zone. This map is modified after Goff et al. (1986) and McDonough et al. (1995).

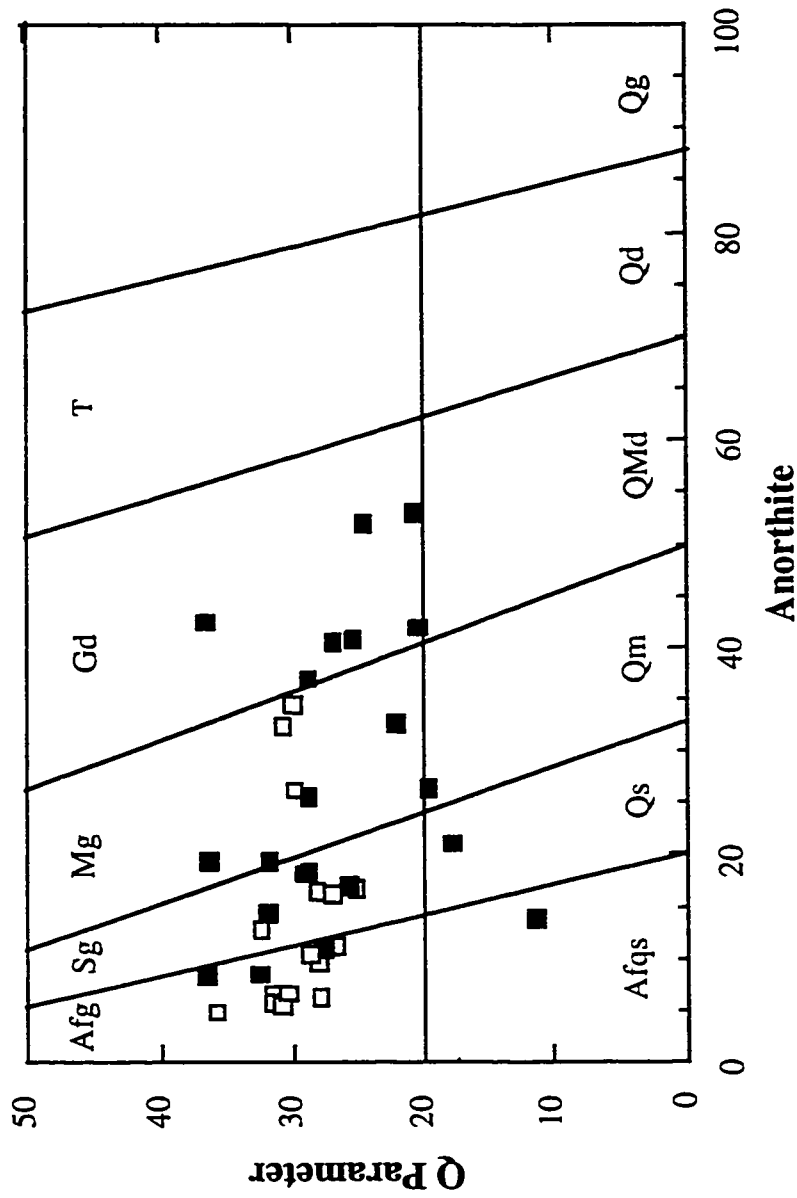


Fig 3. Classification of the TMZ granitoids using the normative equivalent to the IUGS classification developed by Streckeisen and LeMaitre (1979). The two parameters are Anorthite = normative $[An/(Or+An)] \times 100$ and Q parameter = normative $[Q/(Q+Ab+Or+An)] \times 100$. Calculations were conducted using CIPW normative parameters. Open squares represent Western plutons, filled squares represent Eastern plutons. Afq=alkali feldspar granite, Sg=syenogranite, Mg=monzogranite, Gd=granodiorite, T=tonalite, Afqs=alkali feldspar quartzsyenite, Qs=quartzsyenite, Qm=quartz monzonite, QMd= quartz monzodiorite, Qd=quartz diorite, Qg = quartz gabbro.

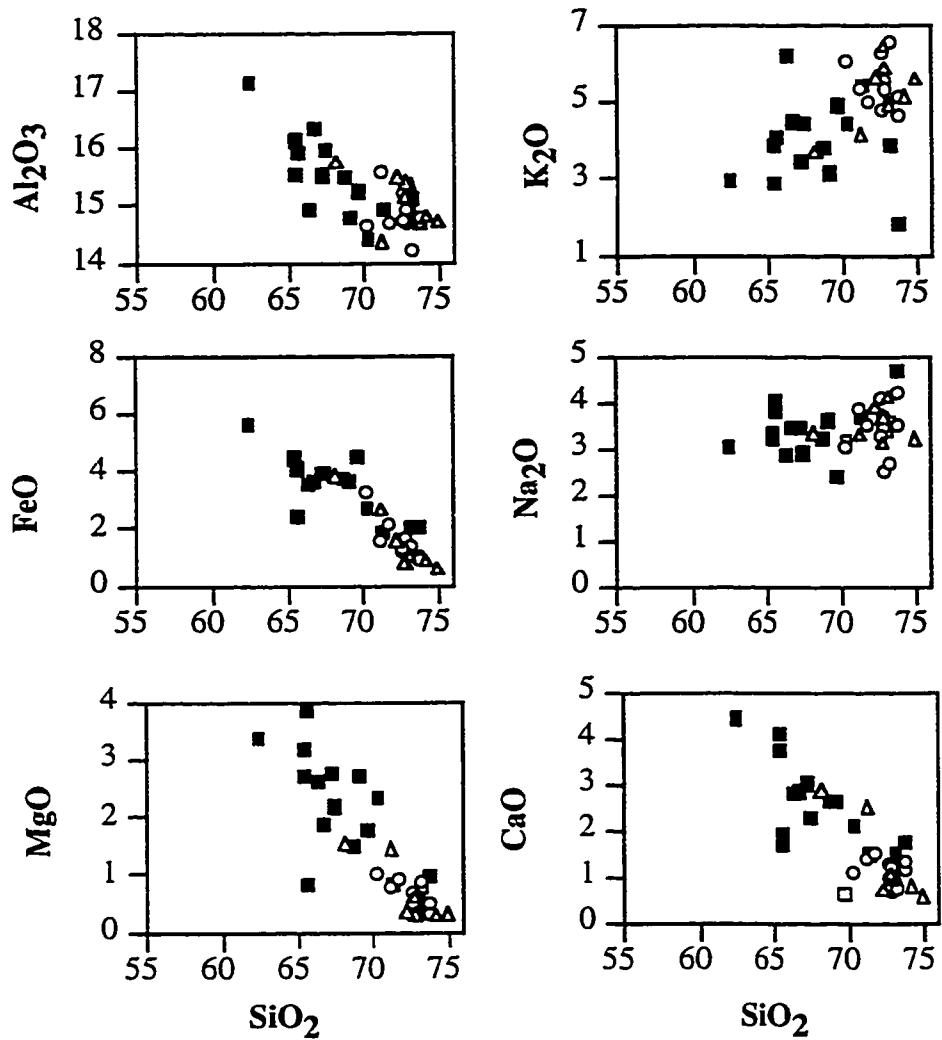


Fig 4: Major element Harker variation diagrams for TMZ granites. filled squares represent Colin Lake and Wylie Lake granites, circles denote Arch Lake granites and the triangles represent Slave granites.

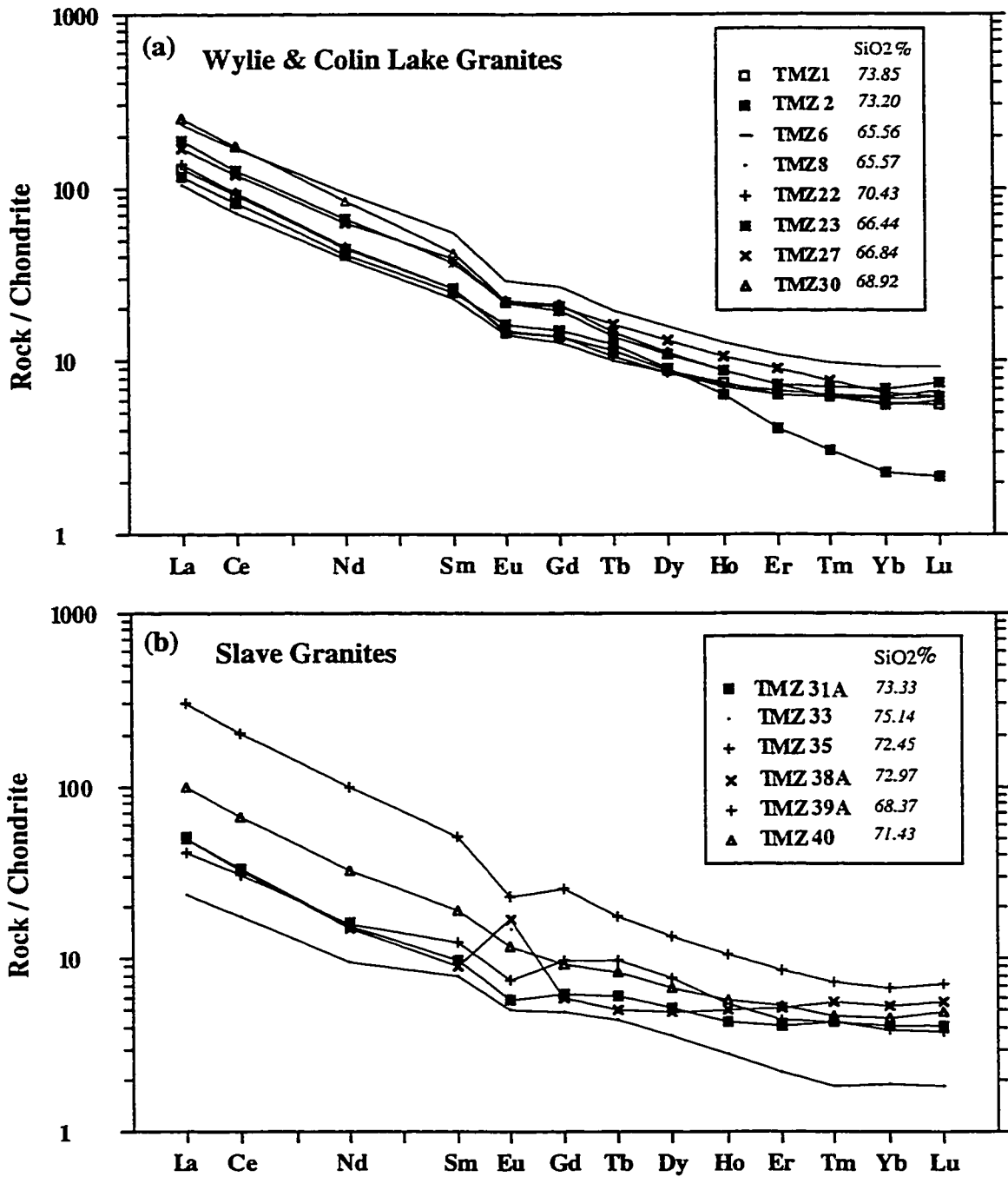


Fig 5. Rare earth element plots for (a) Colin and Wylie Lake granites (b) Slave granites. chondrite normalising values from Boynton (1984).

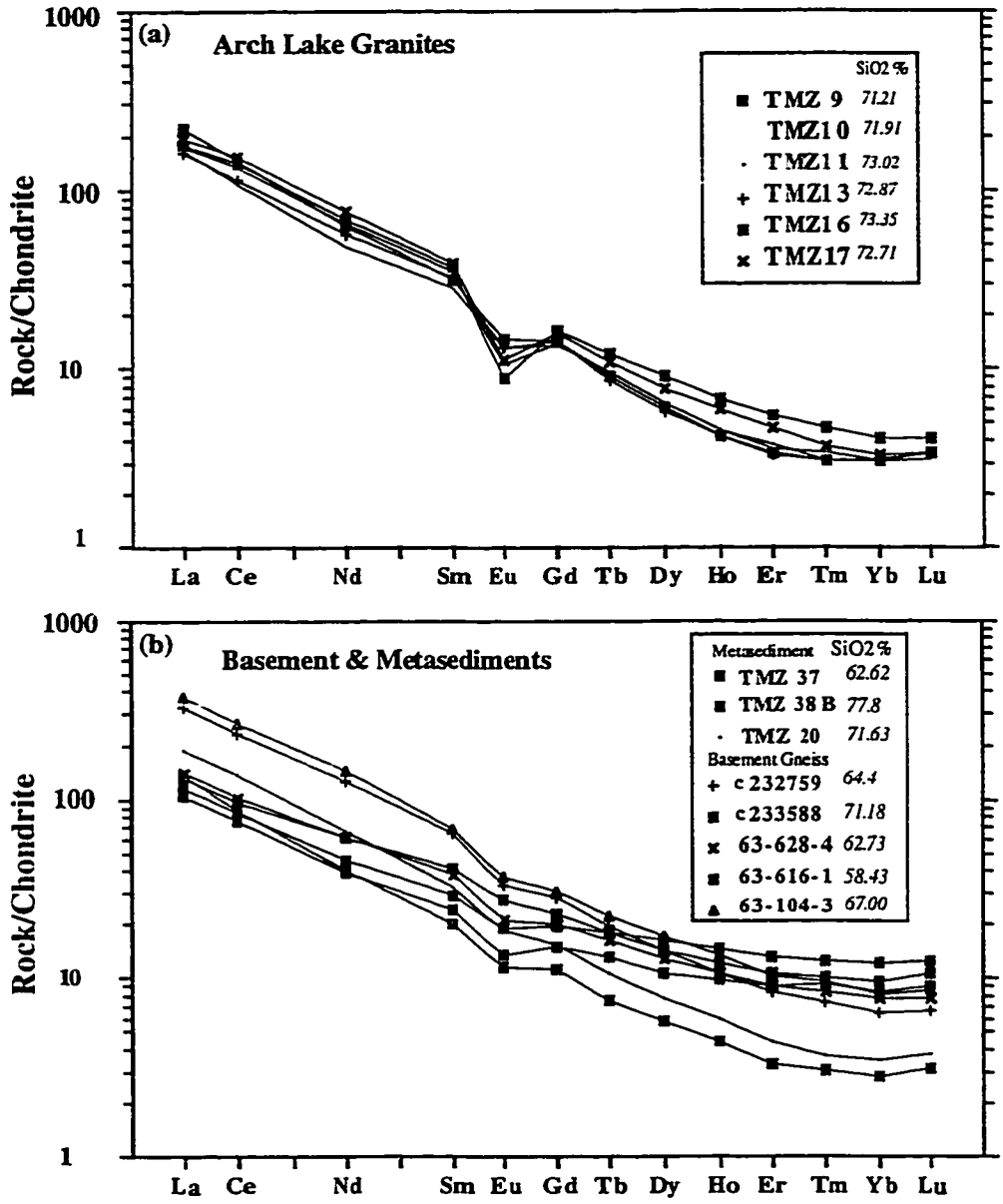


Fig 6. Rare earth element plots for (a) Arch Lake (b) metasediments and basement gneisses from TBC. Chondrite normalisation after Boynton (1984).

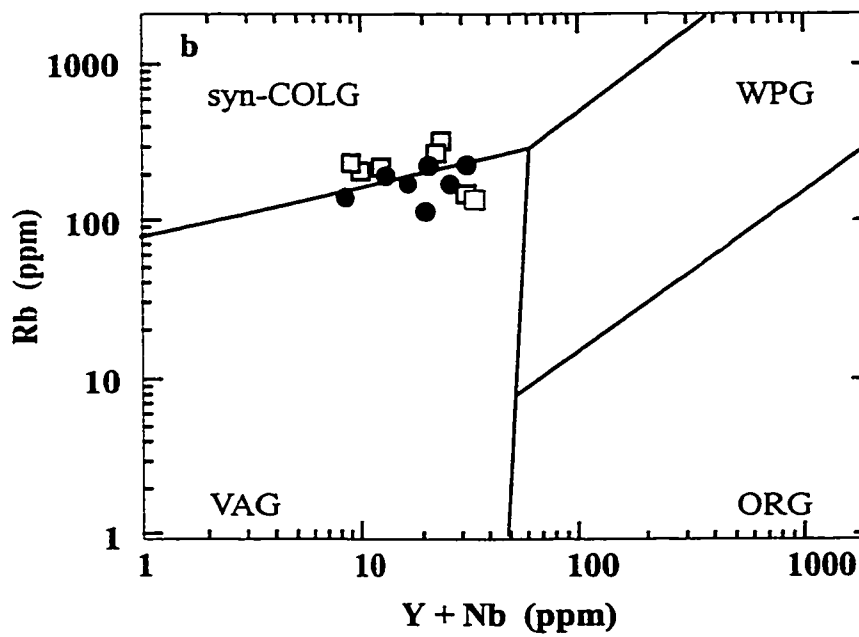
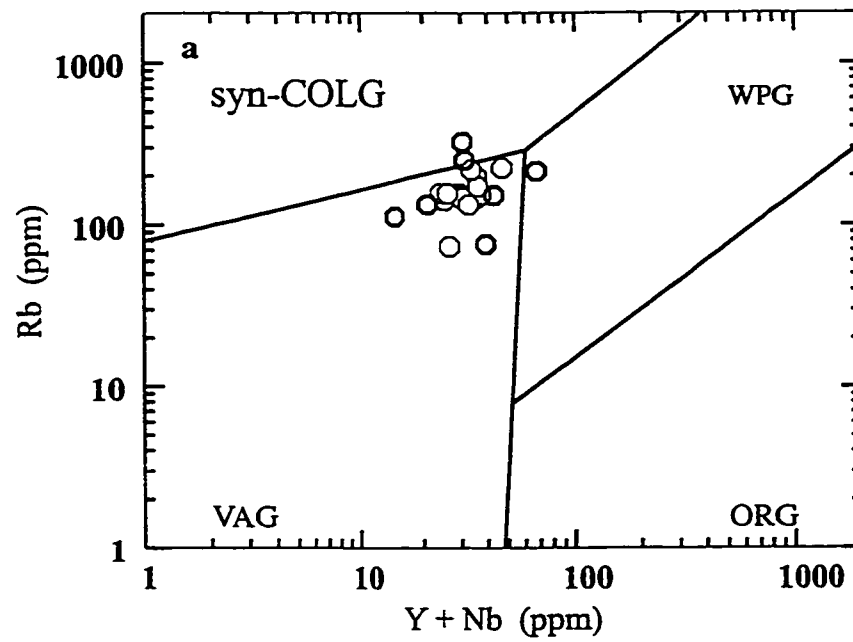


Fig 7. Pearce element plot for (a) Colin Lake and Wylie Lake granites (b) Slave and Arch Lake granites.

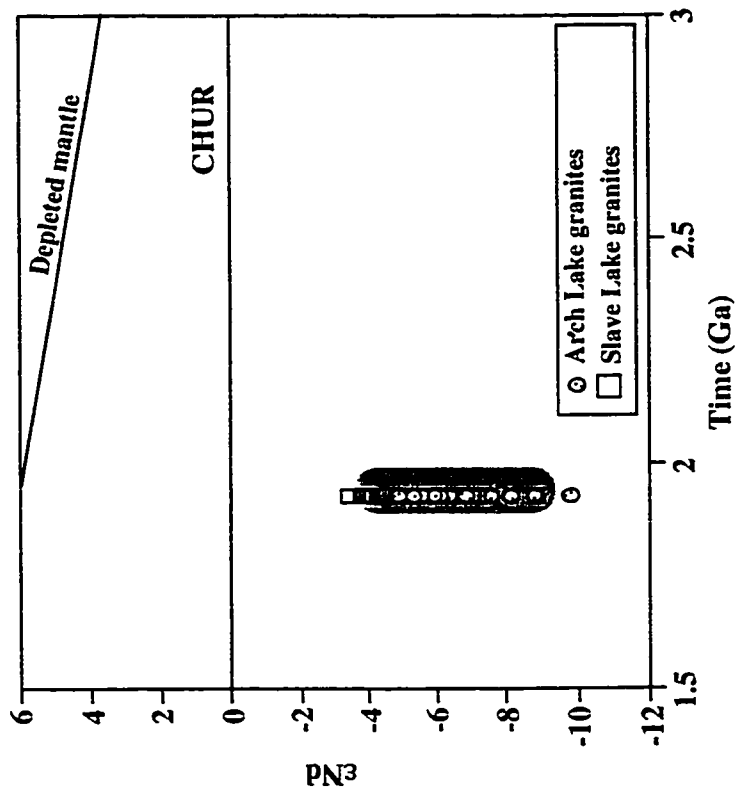


Fig 8. ϵ_{Nd} vs time diagram for the evolution of the Western granites in relation to the shaded area of Pelican Rapid metasediments (Creaser & Chacko pers. comm.) calculated at 1.94 Ga.

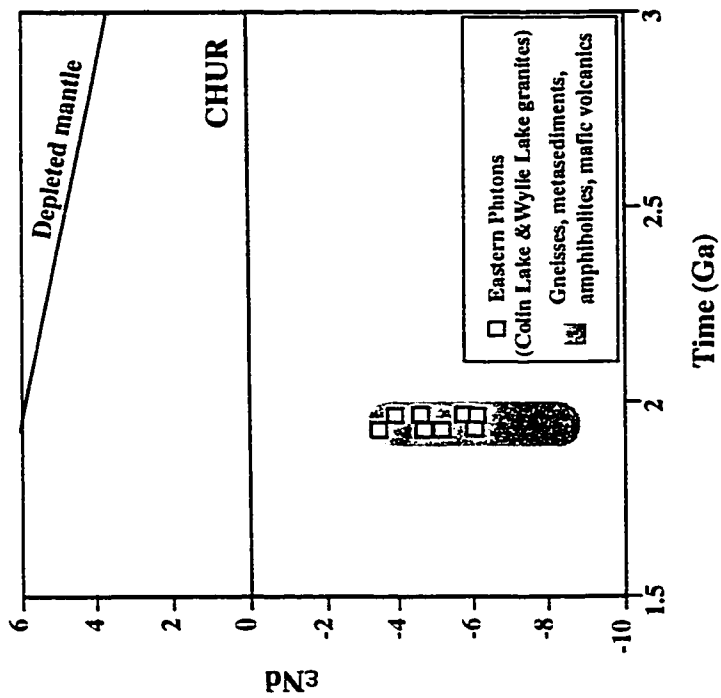


Fig 9. ϵ_{Nd} vs time diagram for the evolution of the eastern TMZ granites in relation to the potential source rocks from which they are derived. The shaded region indicates the range of values of TBC gneisses and metasediments from present study, gneisses of Theriault (1990), amphibolites and mafic volcanics (Theriault 1994, 1997), and mafic granulites (Burwash et al. 1985). All calculations were done at 1.97 Ga. TBC gneissic sample C 233588 with $\epsilon_{Nd}_{1.95} = -17.9$ is not shown on the plot.

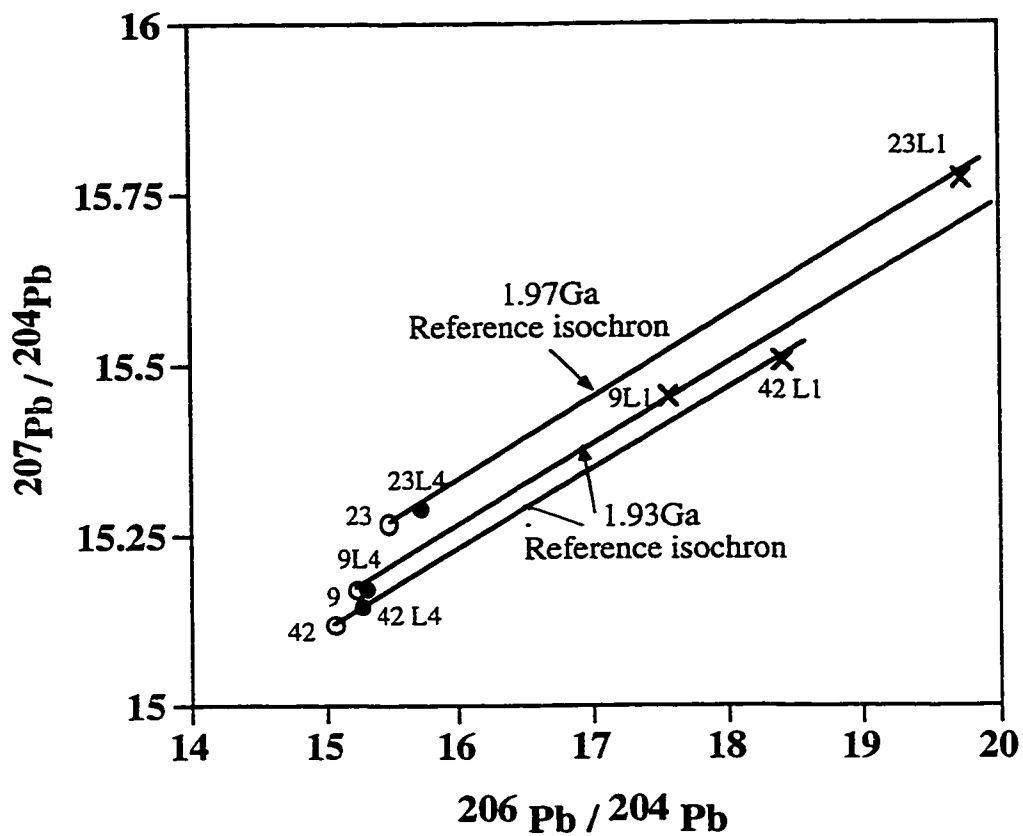


Fig 10. Plot of $^{206}\text{Pb}/^{204}\text{Pb}$ vs. $^{207}\text{Pb}/^{204}\text{Pb}$ for progressive stages of leaching L1, L4 on alkali feldspar separates from samples 9, 23, 42 which are from Arch Lake, Colin Lake and Slave granitoids respectively. Note that there is progressive decrease in the amount of radiogenic Pb with leaching.

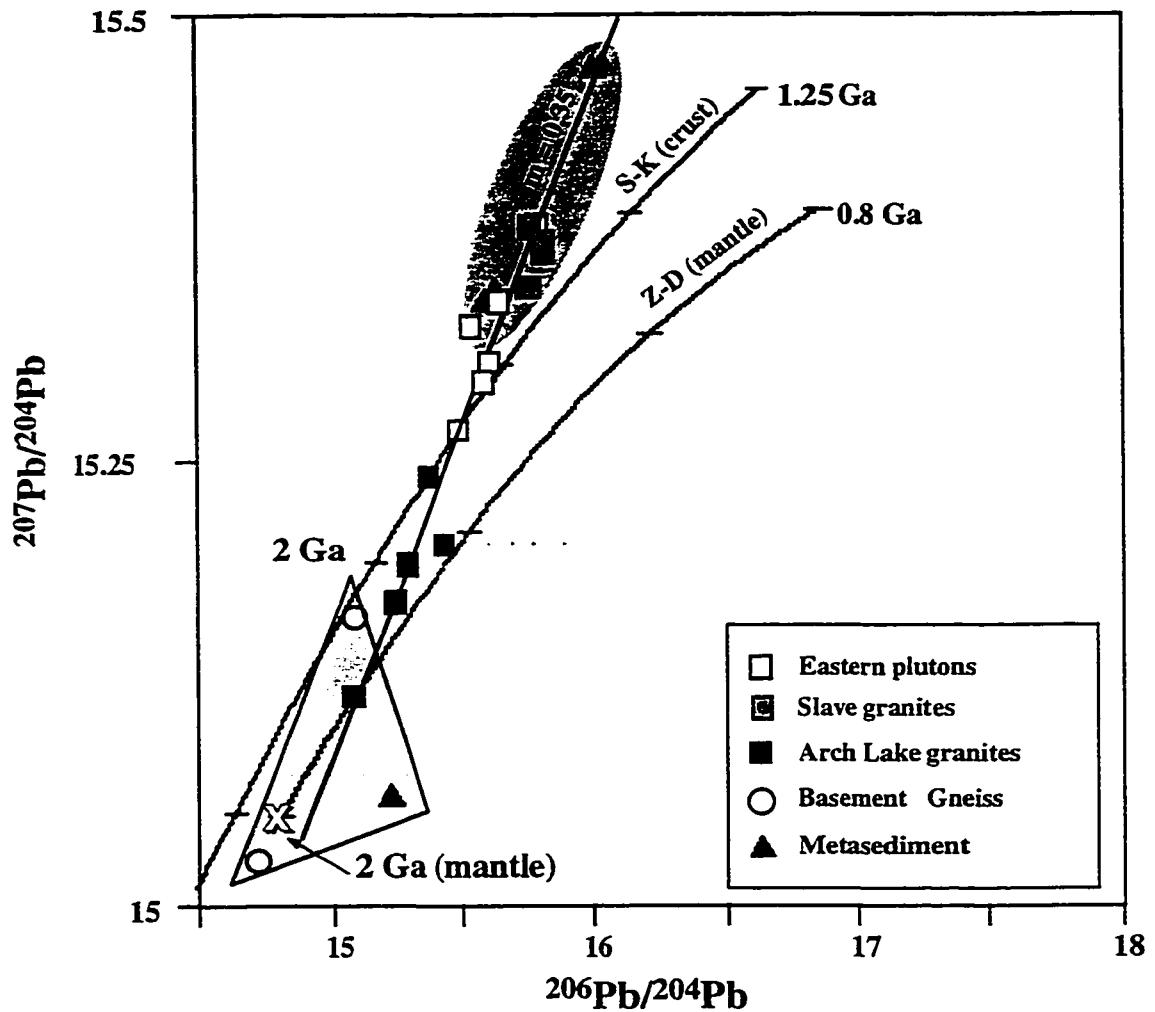


Fig 11. $^{206}\text{Pb}/^{204}\text{Pb}$ vs. $^{207}\text{Pb}/^{204}\text{Pb}$ plot of the TMZ granites in relation to the Stacey & Kramers (1975) crustal evolution curve and Zartman & Doe (1981) mantle evolution curve. Also shown are the reference points of Pb signature at 2 b.y. The grey shaded area represents TMZ metasediments and basement gneisses (present study; unpublished data; Creaser). A possible secondary isochron has a slope of 0.35, the significance of which is described in the text.

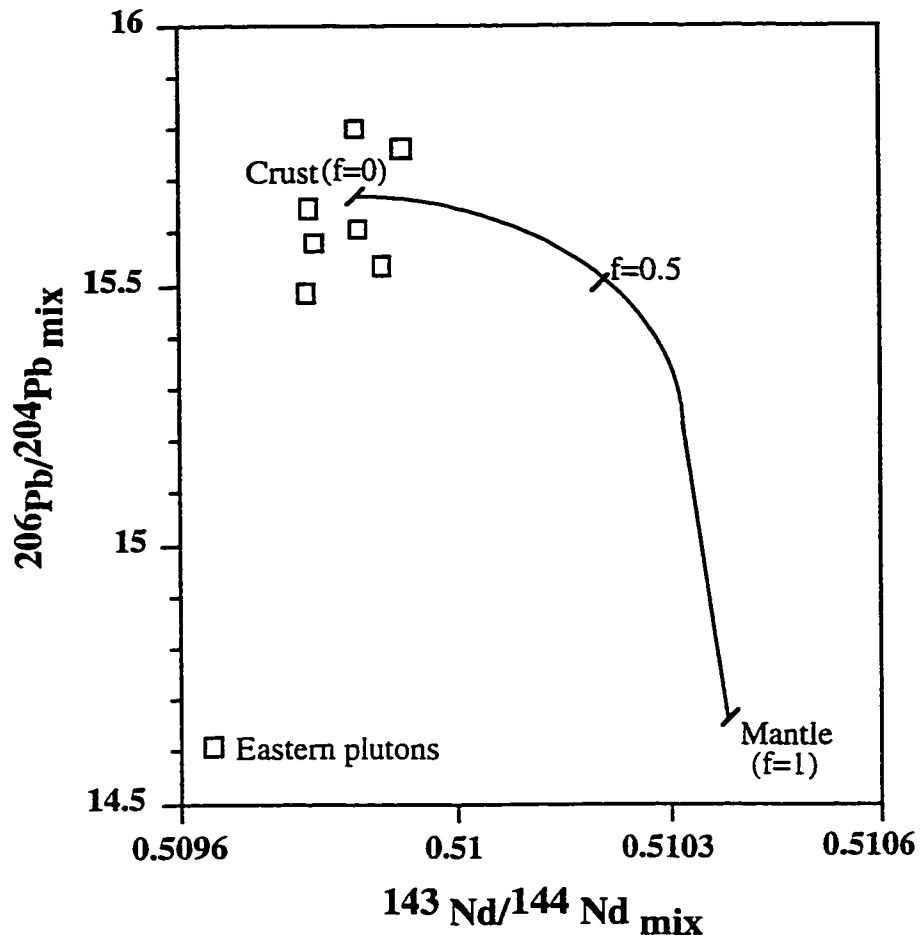


Fig 12. Plot of Colin Lake and Wylie lake granitoids on a $^{206}\text{Pb}/^{207}\text{Pb}$ mix versus $^{143}\text{Nd}/^{144}\text{Nd}$ mix diagram at 1.97 Ga. Mixing hyperbola constructed using equation of Faure 1986. Parameters chosen for metasedimentary crustal end-member ($^{143}\text{Nd}/^{144}\text{Nd}=0.50985$, $\text{Nd}=30$ ppm, $^{206}\text{Pb}/^{204}\text{Pb}=15.67$, $\text{Pb}=28$ ppm [Taylor and McLennan, 1985]. Mantle end member is typical for average island-arc basalts with $\text{Pb}=2.3$ ppm (Meijer, 1976, Woodhead et. al 1993), depleted mantle $^{206}\text{Pb}/^{204}\text{Pb}=14.67$ (Zartman & Doe, 1988), depleted mantle $^{143}\text{Nd}/^{144}\text{Nd}=0.510392$ @ 1.97 Ga. (Faure 1986), $\text{Nd}=25$ ppm (Hawkesworth et. al 1979). The ratio $f = \text{mantle}/(\text{mantle}+\text{crust})$ using the principles of equation 9.1 in Faure (1986).

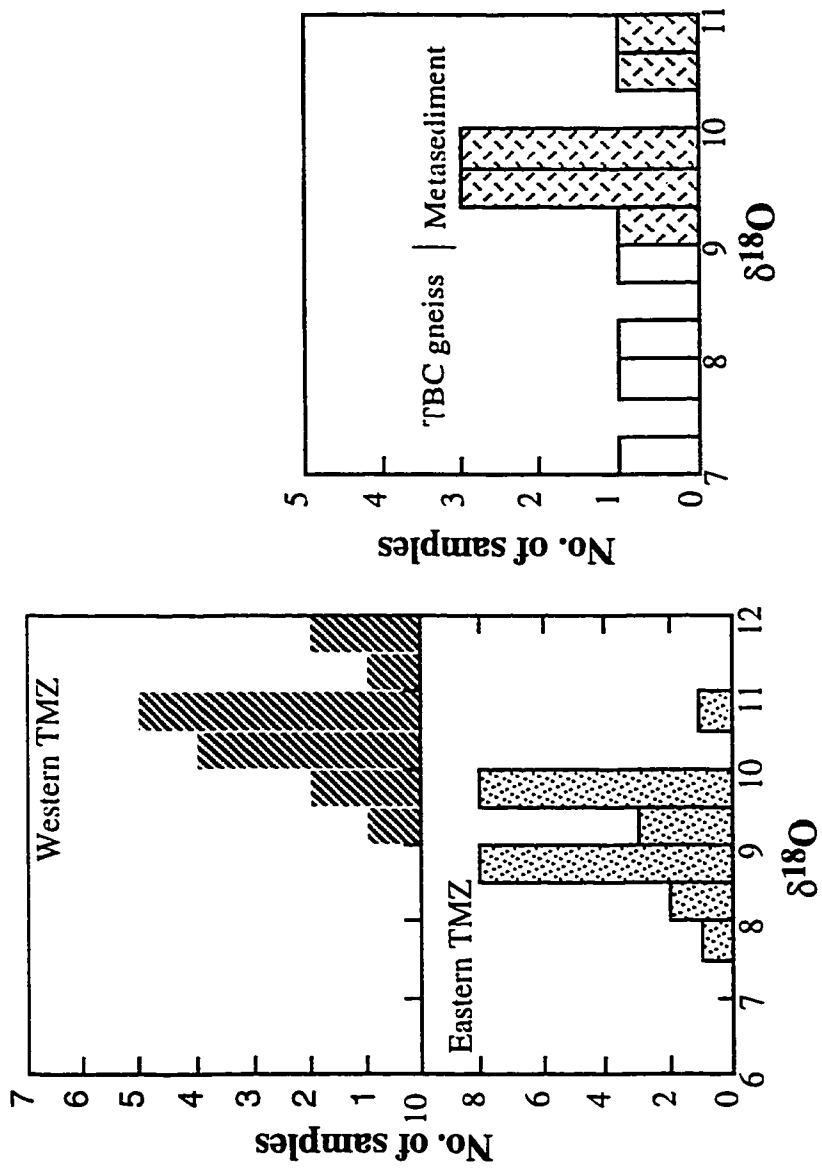
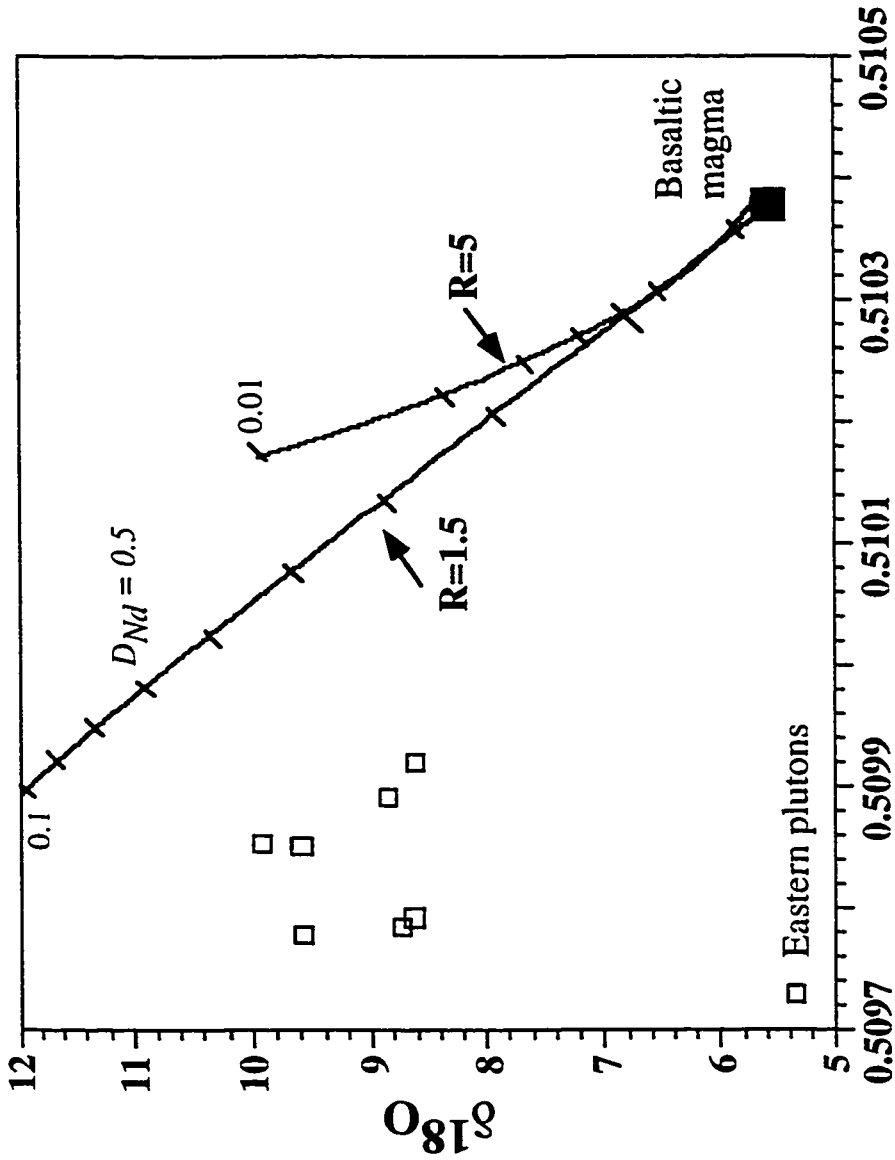


Fig 13. Comparative histograms of oxygen isotopic composition of Eastern and Western TMZ granitoids, TBC felsic gneiss and metasediments



$^{143}\text{Nd}/^{144}\text{Nd} @ 1.97 \text{ Ga}$

Fig 14. Assimilation fractional crystallization plot of Eastern plutons using metasediments as crustal end member ($^{143}\text{Nd}/^{144}\text{Nd} = 0.50985 @ 1.97\text{Ga}$, $\text{Nd} = 30 \text{ ppm}$, $\delta^{18}\text{O} = 12 \text{ per mill}$) and mantle end member ($^{143}\text{Nd}/^{144}\text{Nd} = 0.510392 @ 1.97\text{Ga}$, $\text{Nd} = 2.5\text{ppm}$, $\delta^{18}\text{O} = 5.5\text{per mill}$). Tick marks indicate value of F (melt remaining as a fraction of the original magma). The ratio R denotes mass of cumulates to the assimilated crust. The two different curves correspond to R values of 1.5 and 5 with a D_{Nd} of 0.5.

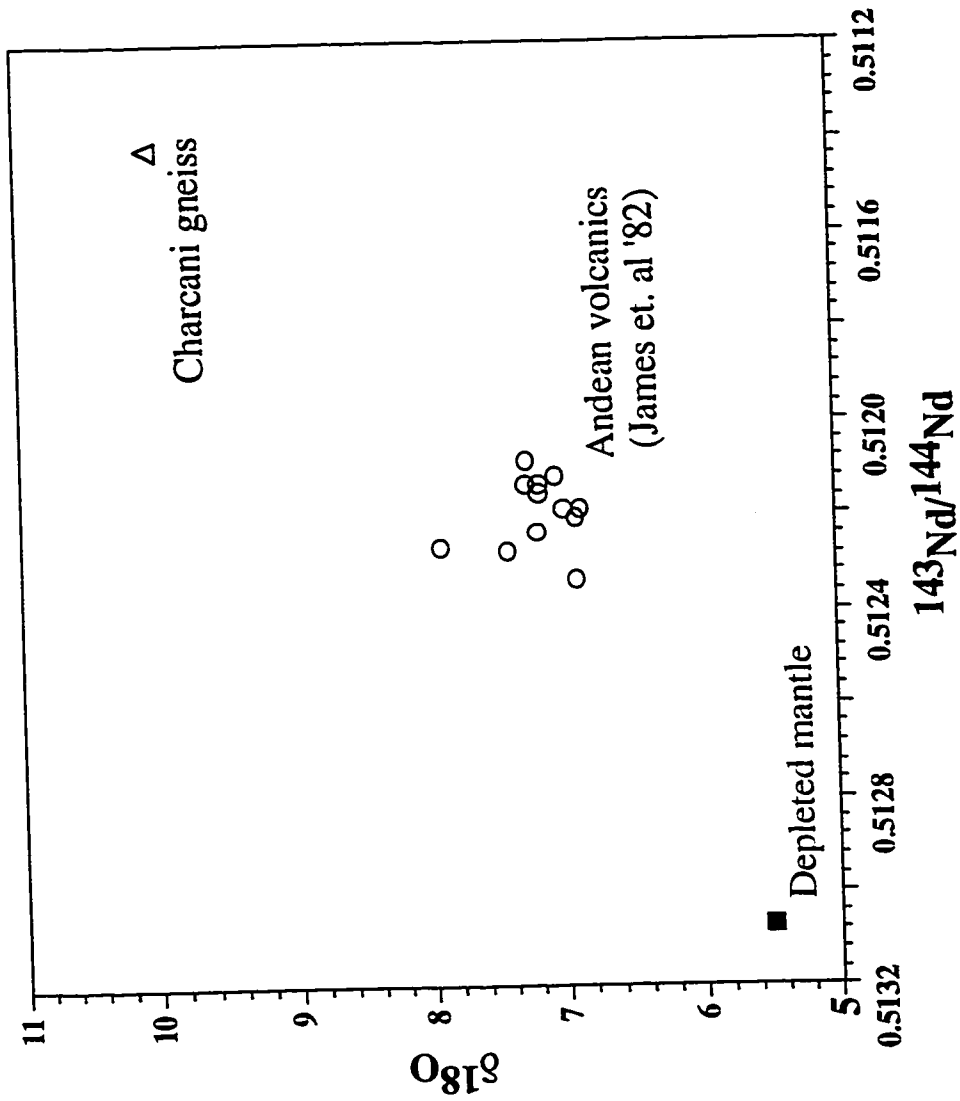


Fig 15. Plot of $^{143}\text{Nd}/^{144}\text{Nd}$ calculated at 65 m.y. versus $\delta^{18}\text{O}$ for calc alkaline Andean volcanics (James et al. 1982). The $^{143}\text{Nd}/^{144}\text{Nd}$ was calculated using a recalculated value of $^{147}\text{Sm}/^{144}\text{Nd} = 0.1119$, using data from Hawkesworth(1972).

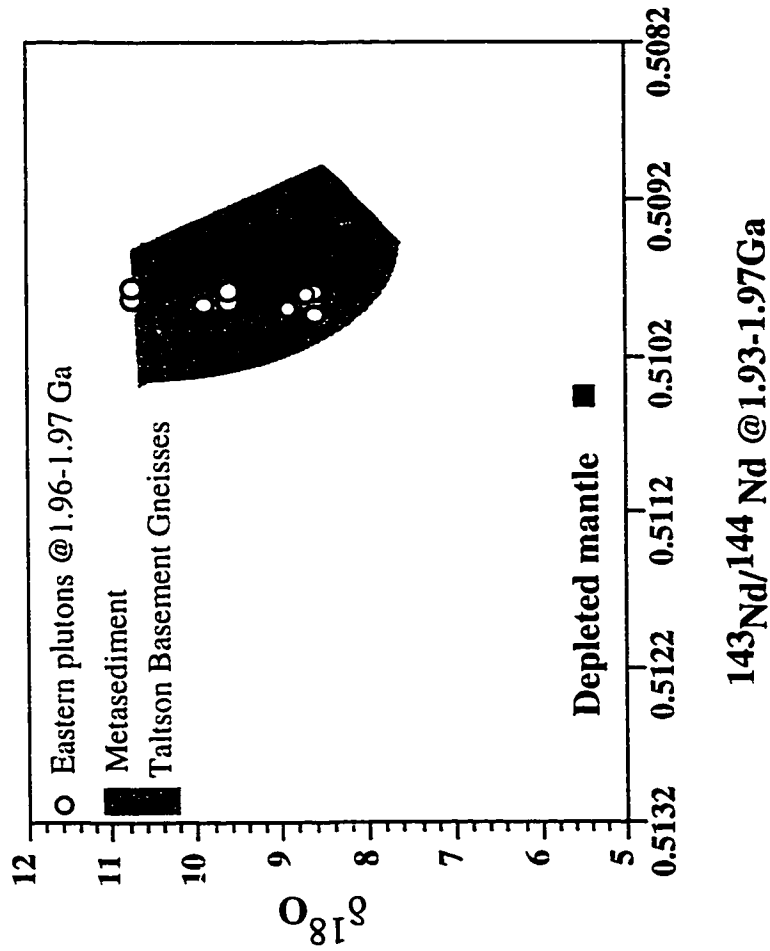


Fig 16. $\delta^{18}\text{O}$ versus $^{143}\text{Nd}/^{144}\text{Nd}$ plot of TMZ granites with respect to the depleted mantle and crustal end-member signature at 1.93 - 1.97 Ga. The crustal end-members in this case being metasediments and Taltson Basement gneisses (TBC).

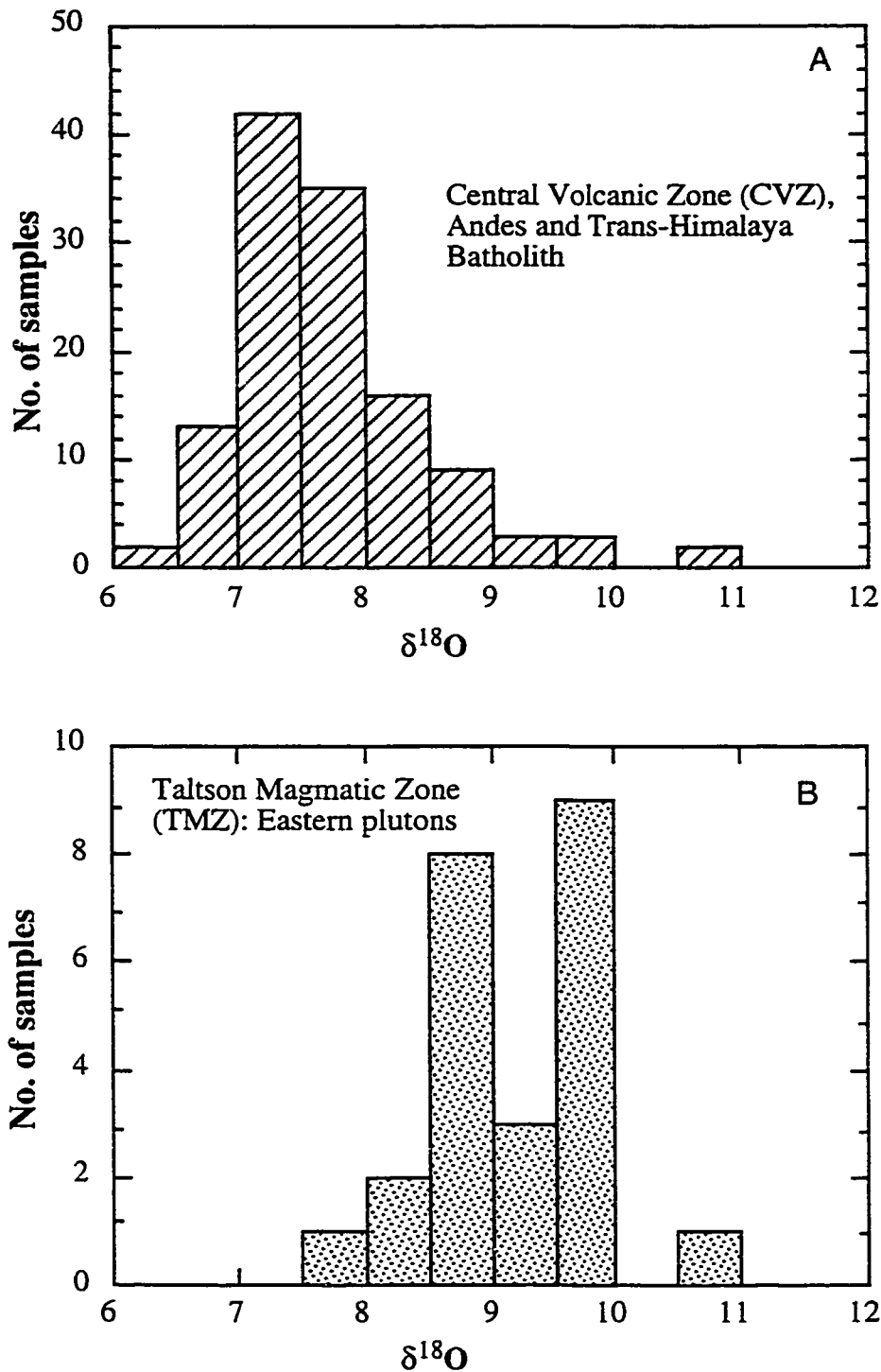


Fig 17. Comparative histograms of oxygen isotopic composition of plutonic and volcanic rocks from the TMZ, CVZ (Andes) and Trans-Himalaya. Data set used are from the present study, James (1982), Longstaffe (1983), Harmon et al. (1984), Debon et al. (1986).

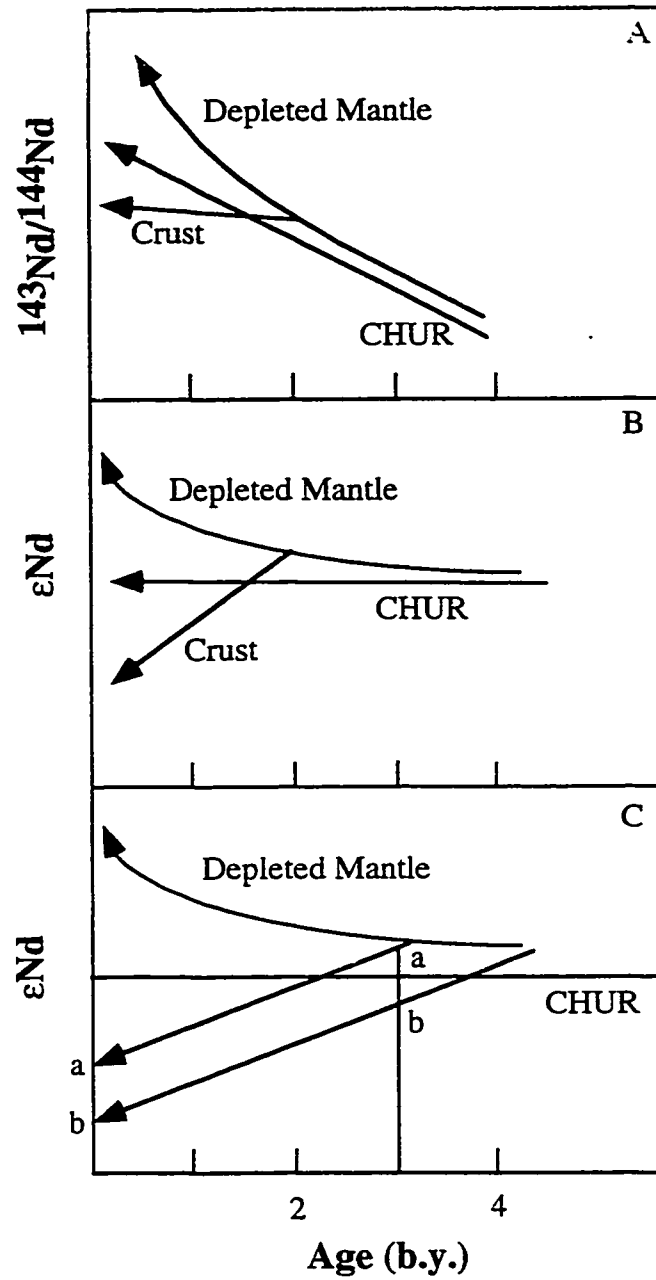


Fig 18. Schematic diagrams for Sm-Nd isotope system and the mantle versus crustal signatures of rock type a and b from present day ϵNd values (C). Refer to Appendix B for details.

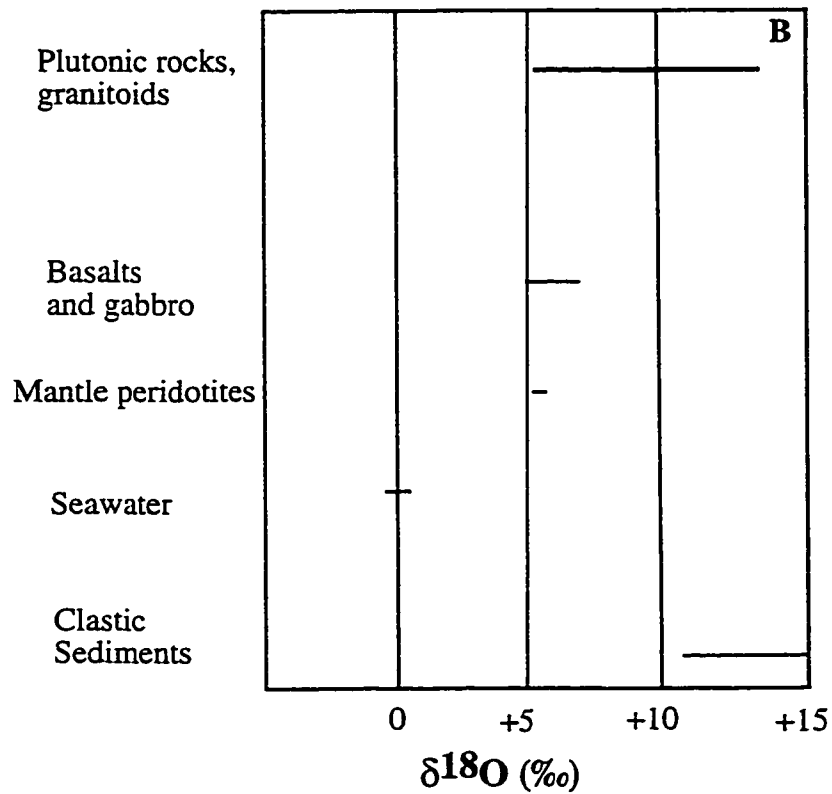
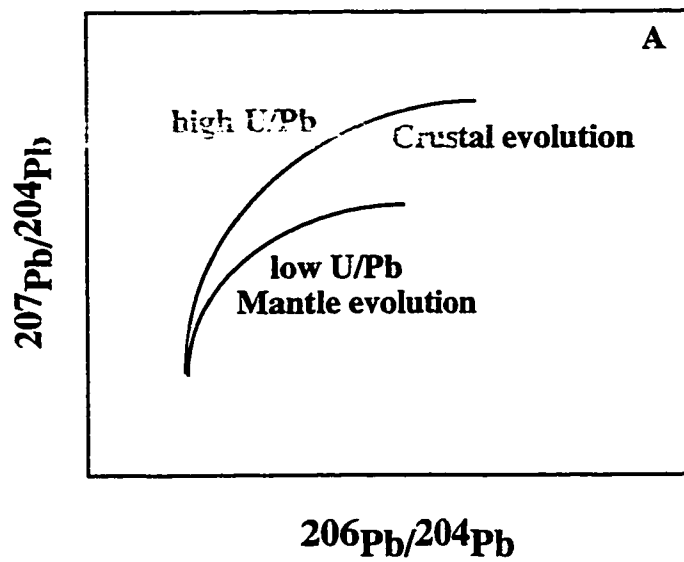


Fig. 19 Schematic diagram for common-Pb isotopic system (A), Range of $\delta^{18}\text{O}$ values for common rock types (B).

REFERENCES

- Baadsgaard, H., Godfrey, J. D. 1967. Geochronology of the Canadian Shield in north eastern Alberta. I. Andrew Lake area. *Canadian Journal of Earth Sciences*, **4**: 541-563.
- Baadsgaard, H., Godfrey, J. D. 1972. Geochronology of the Canadian Shield in north eastern Alberta. II. Charles-Andrew-Colin Lakes area. *Canadian Journal of Earth Sciences*, **9**: 863-881.
- Barker, F., Arth, J.G. 1984. Preliminary results, Central Gneiss Complex of the Coast Range batholith, southeastern Alaska; The roots of a high-K, calc-alkaline arc. *Physics of Earth and Planetary Interiors*, **35**: 191-198.
- Barker, F., Arth, J.G. 1990. Two traverses across the Coast batholith, southeastern Alaska, in Anderson, J.L., ed., The Nature and Origin of Cordilleran magmatism; Boulder, Colorado, *Geological Society of America Memoir* **174**: 395-405.
- Bateman, P.C., Dodge, F.C.W. 1970. Variations in major chemical constituents across the central Sierra Nevada batholith. *Geological Society of America Bulletin*, **81**: 409-420.
- Bostock, H. H., Loveridge, W.D. 1988. Geochronology of the Taltson Magmatic Zone, and its eastern cratonic margin, District of Mackenzie; in Radiogenic Age and Isotopic Studies: Report 2. *Geological Survey of Canada*, Paper **88-2**, 59-65.
- Bostock, H. H., van Breemen, O. 1994. Ages of detrital and metamorphic zircons and monazites from a pre-Taltson magmatic zone basin at the western margin of the Rae province. *Canadian Journal of Earth Sciences*, **31**: 1353-1364.

- Bostock, H.H., van Breemen, O., Loveridge, W.D. 1987. Proterozoic geochronology in the Taltson Magmatic Zone, N.W.T in Radiogenic Age and Isotopic Studies: Report 1. *Geological Survey of Canada*, Paper 87-2: 73-80.
- Bostock, H. H., van Breemen, O., Loveridge, W.D. 1991. Further geochronology of plutonic rocks in northern Taltson magmatic Zone, District of Mackenzie, N.W.T; in Radiogenic Age and Isotopic Studies: Report 4. *Geological Survey of Canada*, Paper 90-2: 67-78.
- Bowring, S.A. 1985. U-Pb geochronology of Early Proterozoic Wopmay orogen, N.W.T., Canada: an example of rapid crustal evolution: Ph.D. thesis, University of Kansas, Lawrence, Kansas.
- Bowring, S.A., Podoseck, F.A. 1989. Nd isotopic evidence for 2.0-2.4 Ga crust in western North America. *Earth and Planetary Science Letters*, **94**: 217-230.
- Bowring, S.A., Grotzinger, J.P. 1992. Implications of new chronostratigraphy for tectonic evolution of Wopmay orogen, northwest Canadian Shield. *American Journal of Science* , **292**:1-21.
- Boynton, W.V. 1984. Cosmochemistry of the rare earth elements: meteorite studies. 67-114, in Henderson, P.(ed) *Rare earth element geochemistry*. Elsevier, 510p.
- Brandon, A., Lambert, R.J. 1994. Crustal melting in the Cordilleran Interior: the Mid-Cretaceous White Creek batholith in the Southern Canadian Cordillera. *Journal of Petrology*. **35-1**:239-269.
- Burg, J.P., Ford, M. 1997. Orogeny through time: an overview in *Geological Society, London, Special Publication* (eds.) Burg, J.P., Ford, M. **121**:1-19.
- Burwash, R.A., Krupicka, J., Basu, A.R., Wagner,P.A. 1985. Resetting Nd and Sr whole rock isochrons from polymetamorphic granulites, northeastern Alberta. *Canadian Journal of Earth Sciences*, **22**: 992-1000.

- Chacko, T. and Creaser, R.A. 1995. Hercynite bearing granites and associated metasedimentary enclaves from the Taltson Magmatic Zone, Alberta, Canada: A Natural example of high temperature pelite melting, in *Origin of Granites and related Rocks, Third Hutton Symposium Abstracts, USGS Circular 1129*: 32-33.
- Chacko, T., Creaser, R. A., Poon, D. 1994. Spinel + quartz granites and associated metasedimentary enclaves from the Taltson magmatic zone, Alberta, Canada: a view into the root zone of a high temperature S-type granite batholith. *Mineralogical Magazine*, **8A**: 161-162.
- Chappel, B.W., White, A.J.R. 1974. Two contrasting granite types. *Pacific Geology*, **8**: 173-174.
- Clayton, R.N. Mayeda, T.K. 1963. The use of bromine pentafluoride in the extraction of oxygen from oxides and silicates for isotopic analysis. *Geochimica et Cosmochimica Acta*, **27**: 43-52.
- Condie, K.C. 1997. Plate Tectonics and Crustal evolution, Fourth edition. Butterworth Heinemann. 282p.
- Crawford, M.B., Searle, M.P. 1992. Field relationships and geochemistry of precollisional (India-Asia) granitoid magmatism in the central Karakorum, northern Pakistan. *Tectonophysics*, **206**: 171-192.
- Creaser, R. 1995. Radiogenic Isotopes in granitic systems: Studies of melting and mixing at the source, in *Origin of Granites and related Rocks, Third Hutton Symposium Abstracts, USGS Circular 1129*: 38-39.
- Creaser, R., Erdmer, P., Stevens, R.A., Grant, S.L. 1997. Tectonic affinity of Nisutlin and Anvil assemblage strata from the Teslin tectonic zone, northern Canadian Cordillera: constraints from neodymium isotope and geochemical evidence. *Tectonics*, **16**: 107-121.

- Cumming, G.L., and Krstic, D. 1987. Geochronology at the Namew Lake Cu-Ni deposit, Flin Flon area, Manitoba, Canada: a Pb-Pb study of whole rocks and ore minerals. *Canadian Journal of Earth Sciences*, **28**:1328-1339.
- Debon, F., Le Fort, P., Sheppard, S. M.F., & Sonet, J. 1986. The Four Plutonic Belts of the Transhimalaya-Himalaya: a Chemical, Mineralogical, Isotopic, and Chronological Synthesis along a Tibet-Nepal Section. *Journal of Petrology*, **27** Part 1: 219-250.
- DePaolo, D.J. 1980. Neodymium isotopes in the Colorado Front Range and crust-mantle evolution in the Proterozoic. *Nature*, **291**: 193-196.
- DePaolo, D.J. 1981. Trace-element and isotopic effects on combined wallrock assimilation and fractional crystallisation. *Earth and Planetary Science Letters*, **53**: 189-202.
- DePaolo, D.J. 1988. Neodymium Isotope Geochemistry, An Introduction. *Springer Verlag*. 187p.
- Driver, L.A., Creaser, R., Chacko, T., Erdmer, P. 1998. Petrogenesis of the Cretaceous Cassiar batholith, Yukon-B.C. Canada. In Cook, F. and Erdmer, P. (compilers) Slave and Northern Cordillera (SNORCLE) and Cordilleran tectonics workshop meeting, Simon Fraser University, *LITHOPROBE Report No.64*, 158-164.
- Drummond, M.S., Defant, M.J., Kepezhinskas, P.K. 1996. Petrogenesis of slab derived trondhjemite-tonalite-dacite/adakite magmas. *Transactions of Royal Society of Edinburgh: Earth Sciences*, **78**: 205-216.
- Farmer, L.G. 1992. Magmas as tracers of lower crustal composition: an isotopic approach, in Kay, R., Fountain, D., Arculus, R.J (eds.) Lower continental crust, Pergamon Press, 363-390.
- Faure, G. 1986. Principles of Isotope Geology (2nd edn.). 589pp.

- Feng, R., Kerrich, R. 1990. Geochemistry of fine grained clastic sediments in the Archean Abitibi greenstone belt, Canada: Implications for provenance and tectonic setting. *Geochimica et Cosmochimica Acta*, **54**: 1061-1081.
- Feng, R., Kerrich, R., Maas, R. 1993. Geochemical , oxygen, and neodymium isotopic composition of metasediments from the Abitibi greenstone belt and Pontiac subprovince, Canada: Evidence for ancient crust and Archean terrane juxtaposition. *Geochimica et Cosmochimica Acta*, **57**: 641-658.
- Gibb, R.A., & Thomas, M.D. 1977. The Thelon Front: a cryptic suture in the Canadian Shield? *Tectonophysics*, **38**: 211-222.
- Godfrey, J.D. 1961. Geology of the Andrew Lake, north district; Alberta Research Council, Preliminary Report 58-3, 32p.
- Godfrey, J.D. 1963. Geology of the Andrew Lake, south district; Alberta Research Council, Preliminary Report 61-2, 30p.
- Godfrey, J.D. 1986. Geology of the Precambrian Shield in northeastern Alberta; Alberta Research Council Map 1986-1, scale 1:250 000.
- Godfrey, J.D., Langenberg, C.W. 1978. Metamorphism in the Canadian Shield of northeastern Alberta; in *Metamorphism in the Canadian Shield*, (eds.) Fraser, J., Heywood, W.W., *Geological Survey of Canada*, Paper 78-10: 129-138.
- Goff, S.P., Godfrey, J.D., & Holland, J.G. 1986. Petrology and geochemistry of the Canadian shield of northeastern Alberta; *Alberta Research Council*, Bulletin 51: 60p.
- Goldstein, S.L., O’Nions, R.K., Hamilton, P.J. 1984. A Sm-Nd isotopic study of atmospheric dusts and particulates from major river systems. *Earth and Planetary Science Letters*, **70**: 221-236.
- Grover, T.W., McDonough, M.R., McNicoll, V.J. 1993. Preliminary report of the metamorphic geology of Taltson magmatic zone, Canadian Shield, northeastern

- Alberta; in Current Research, Part C; *Geological Survey of Canada*, Paper 93-1C: 233-238.
- Grover, T.W., Pattison, D.R.M., McDonough, M.R., McNicoll, V.J. 1997. Tectonometamorphic evolution of the southern Taltson Magmatic Zone and associated shear zones, Northeastern Alberta. *Canadian Mineralogist*, **35**: 1051-1067.
- Hanson, G.N. 1980. Rare earth elements in petrogenetic studies of igneous systems. *Annual Review of Earth and Planetary Sciences*, **8**: 371-406.
- Harmon, R.S., Barriero, B.A., Moorbath, S., Hoefs, J., Francis, P.W., Thorpe, R.S., Deruelle, B., McHugh, J., Viglino, J.A. 1984. Regional O-Sr-, and Pb-isotope relationships in late Cenozoic calc-alkaline lavas of the Andean Cordillera. *Journal of Geological Society London*, **141**:803-822.
- Hawkesworth, C.J., Norry, M.J., Roddick, J.C., Baker, P.E. 1979. $^{143}\text{Nd}/^{144}\text{Nd}$, $^{87}\text{Sr}/^{86}\text{Sr}$, and incompatible element variations in calc-alkaline andesites and plateau lavas from South America. *Earth and Planetary Science Letters*, **42**: 45-57.
- Hawkesworth, C.J., O'Nions, R.K., Arculus, R.J. 1979. Nd and Sr isotope geochemistry of Island arc volcanics, Grenada, Lesser Antilles. *Earth and Planetary Science Letters*, **45**: 237-248.
- Hildebrand, R.S., Hoffman, P.F., Bowring, S. A. 1987. Tectono-magmatic evolution of the 1.9 Ga Great Bear Magmatic Zone, Wopmay Orogen, Northwestern Canada. *Journal of Volcanology and Geothermal Research*, **32**: 99-118.
- Hildreth, W., Moorbath, S. 1988. Crustal contributions to arc magmatism in the Andes of Central Chile. *Contributions to Mineralogy and Petrology*, **98**: 455-489.

- Hirn, A., Sapin, M., Lepine, J.C., Diaz, J., Jiang, M. Increase in melt fraction along a north-south traverse below the Tibetan plateau; evidence from seismology. *Tectonophysics*, **273**: 17-30.
- Hoefs, J. 1997. Stable Isotope Geochemistry. *Springer Verlag*, 201p.
- Hoffman, P.F. 1987. Continental transform tectonics: Great Slave Lake shear zone (ca. 1.9 Ga), northwest Canada. *Geology*, **15**: 785-788.
- Hoffman, P. F. 1988. United Plates of America, The Birth of a Craton; *Annual Review of Earth and Planetary Sciences*, **14**: 757-773.
- Hoffman, P. F., 1989. Precambrian geology and tectonic history of North America; in The Geology of North America- An overview, (ed.) A Bally and A.R. Palmer; *Geological Society of America*, The Geology of North America, v.A: 487-512.
- Hooper, P.R., Johnson, D.M., Conrey, R.M. 1993. Major and trace element analysis of rocks and minerals by X-ray spectrometry, Open file report, Washington State University, Pullman, Washington.
- James, D.E. 1971a. Andean crustal and upper mantle structure. *Journal of Geophysical Research*, **6**: 3246-3271.
- James, D.E. 1981. The combined use of oxygen and radiogenic isotopes as indicators of crustal contamination. *Annual Review of Earth and Planetary Sciences*, **9**: 311-344.
- James, D.E. 1982. A combined O, Sr, Nd, and Pb isotopic and trace element study of crustal contamination in Central Andean lavas, I. Local geochemical variations. *Earth and Planetary Science Letters*, **57**: 47-62.
- James, D.E. 1984. Quantitative models for crustal contamination in the central and northern Andes in *Andean Magmatism* (eds.) Harmon, R.S., Barriero, B.A. 124-138.

- Knaack, C., Cornelius, S., Hooper, P. 1994. Trace element analyses of rocks and minerals by ICP-MS. GeoAnalytical Laboratory, Washington State University, Pullman, Washington.
- Langenberg, C.W., & Nielsen, P.A., 1982. Polyphase Metamorphism in the Canadian Shield of northeastern Alberta; *Alberta Research Council, Bulletin 42*: 80p.
- Longstaffe, F.J., Clark, A., McNutt, R.H., Zentilli, M. 1983. Oxygen isotopic compositions of Central Andean plutonic and volcanic rocks, latitudes 26°-29° south. *Earth and Planetary Science Letters*, **64**: 9-18.
- Lugmair, G.W., Galer, S.J.G. 1992. Age and isotope relationships among the angrites Lewis Cliff 86010 and Angra dos Reis. *Geochimica et Cosmochimica Acta*, **56**: 1673 -1694.
- Martin, H. 1986. Effect of steeper Archean geothermal gradient on geochemistry of subduction zones. *Geology*, **14**, 753-756.
- McDonough, M.R., Grover, T.W., McNicoll, V.J., Lindsay, D.D. 1993. Preliminary report of the geology of the southern Taltson magmatic zone, northeastern Alberta; in Current research, Part C: *Geological Survey of Canada*, Paper 93-1C: 221-232.
- McDonough, M.R. 1994. $^{40}\text{Ar}/^{39}\text{Ar}$ and K-Ar age constraints on shear zone evolution, southern Taltson Magmatic Zone, Northeastern Alberta. in Ross, G.M., (editor) *Alberta Basement Transects Workshop, Lithoprobe Report #37, LITHOPROBE Secretariat, University of British Columbia*, 254- 266.
- McDonough, M.R., McNicoll, V.J., Schetselaar, E.M. 1995. Age and kinematics of crustal shortening and escape in a two sided oblique slip collisional and magmatic orogen, paleoproterozoic Taltson Magmatic Zone, northeastern Alberta, in Ross, G.M., (editor) *Alberta Basement Transects Workshop, Lithoprobe Report #47, LITHOPROBE Secretariat, University of British Columbia*, 264-309.

- McDonough, M.R., and McNicoll, V.J. 1997. U-Pb age constraints on the timing of deposition of the Waugh Lake and Burntwood (Athabasca) groups, southern Taltson magmatic zone, northeastern Alberta. in Radiogenic Age and Isotopic Studies: Report 10. *Geological Survey of Canada, Current Research 1997-F* : 101-111.
- McLennan, S.M., Hemming, S.R., Taylor, S.R., Eriksson, K.A. 1995. Early Proterozoic crustal evolution: Geochemical and Nd-Pb isotopic evidence from metasedimentary rocks, southwestern North America. *Geochimica et Cosmochimica Acta*, **59**:1153-1177.
- McNicoll, V.J., McDonough, M., Grover, T. 1993. Preliminary U-Pb geochronology of the Southern Taltson Magmatic Zone, northeastern Alberta. in Ross, G.M., (editor) *Alberta Basement Transects Workshop, Lithoprobe Report #31, LITHOPROBE Secretariat, University of British Columbia*, 129-130.
- Meijer, A. 1976. Pb and Sr isotopic data bearing on the origin of volcanic rocks from the Mariana island-arc system. *Geological Society of America Bulletin*. **87**: 1358-1369.
- Miller, C.F., Barton, M.D., 1990. Phanerozoic plutonism in the Cordillera interior, U.S.A. In Kay, S.A. and Rapela, C.W. (eds.) *Plutonism from Antarctica to Alaska*. Boulder, Colorado: *Geological Society of America Special Paper*, **241**: 213-231.
- Neil, E.A., Houseman, G.A. 1997. Geodynamics of the Tarim Basin and the Tian Shan in central Asia. *Tectonics*, **16**: 571-584.
- Nielsen, P. A., Langenberg, C. W., Baadsgaard, H., Godfrey, J. D. 1981. Precambrian Metamorphic Conditions and Crustal Evolution, Northeastern Alberta, Canada. *Precambrian Research*, **16**: 171-193.

- Nielsen, R.L. 1989. Phase equilibria constraints on liquid lines of descent generated by paired assimilation and fractional crystallization: trace elements and Sr and Nd isotopes. *Journal of Geophysical Research.*, **94**: 787-794.
- Patchett, P.J. 1992. Isotopic studies of Proterozoic crustal growth and evolution, in *Kroner, A.(ed) Proterozoic Crustal Evolution, Elsevier*, 481-508.
- Patchett, P.J. 1986. Nd isotopes and tectonics of 1.9-1.7Ga crustal genesis. *Earth and Planetary Science Letters*, **78**: 329-338.
- Patino Douce, A.E., Humphreys, E.D., Johnston, A.D., 1990. Anatexis and metamorphism in tectonically thickened continental crust exemplified by the Sevier hinterland, western North America. *Earth and Planetary Science Letters*, **97**: 290-315.
- Pearce, J.A., Harris, N.B.W., Tindle, A.G. 1984. Trace element discrimination diagrams for tectonic interpretations of granitic rocks. *Journal of Petrology*, **25** (4): 956-983.
- Pitcher, W.S., 1993. The Nature and Origin of Granite. Blackie Academic & Professional. 321p.
- Roddick, J.A. 1983b. Geophysical review and the composition of the Coast Plutonic Complex, south of latitude 55°N: in Roddick, J.A. (ed) Circum-Pacific plutonic terranes: *Geological Society of America Memoir* **159**: 195-211.
- Rogers, J.J.W. 1993. A History of the Earth. Cambridge University Press. 312p.
- Ross, G.M., Parrish, R.R., Villeneuve, M.E., Bowring, S.A., 1991. Geophysics and geochronology of the crystalline basement of the Alberta Basin, western Canada. *Canadian Journal of Earth Sciences*, **28**: 512-522.
- Silver, L.T., Taylor, H.P., Chappell, B.W. 1979. Some petrological, geochemical, and geochronological observations of the Peninsular Ranges batholith near the

- international border of the U.S.A. and Mexico, in Abbott, P.L., and Todd, V.R., (eds) Mesozoic crystalline rocks; *Geological Society of America annual meeting guidebook*: San Diego, California, San Diego State University, 83-110.
- Stacey, J. S., Kramers, J.D. 1975. Approximation of terrestrial lead isotope evolution of a two stage model. *Earth and Planetary Science Letters*, **26**: 207-221.
- Streckeisen, A.L. and LeMaitre, R.W. 1979. Chemical approximation to modal QAPF classification of the igneous rocks. *Neues. Jahrb.Mineral.Abh*, **136**: 169-206.
- Taylor, H.P. 1980. The effects of assimilation of country rocks by magmas on $^{18}\text{O}/^{16}\text{O}$ and $^{87}\text{Sr}/^{86}\text{Sr}$ systematics in igneous rocks. *Earth and Planetary Science Letters*, **47**: 243-254.
- Taylor, H.P., Epstein, S. 1962. Relationship between $\text{O}^{18}/\text{O}^{16}$ ratios in coexisting minerals of igneous and metamorphic rocks. *Geological Society of America Memoir* , **73**: 461-480.
- Taylor, H.P. and Sheppard, S.M.F. 1986. Igneous Rocks: I. Process of isotopic fractionation and isotope systematics , in Valley, J.W., Taylor, H.P., O'Neil, J.R. (eds.) Stable isotopes in High temperature geological processes: reviews in Mineralogy, 16, *Mineralogical Society of America* , Washington D.C. 227-271, 570p.
- Theriault, R.J. 1992. Overview of the geochemistry and petrology of the Taltson granites: segment of a 1.9-2.0 Ga 3200 km magmatic belt in western Canada. in Ross, G.M., (editor) *Alberta Basement Transects Workshop (March 4-5), Workshop Report #28, LITHOPROBE Secretariat, University of British Columbia*, 118.

- Theriault, R.J. 1992. Nd isotopic evolution of the Taltson Magmatic Zone, Northwest territories, Canada : Insights into early Proterozoic accretion along the Western margin of the Churchill Province. *Journal of Geology*, **100**: 465-475.
- Theriault., R.J., 1994. Nd isotopic evidence for Protopaleozoic pre-Taltson Magmatic Zone (1.99-1.90 Ga) rifting of the western Churchill Province. *in Ross, G.M., (editor) Alberta Basement Transects Workshop (February 14-15), Lithoprobe Report #37, LITHOPROBE Secretariat, University of British Columbia, 267-269.*
- Theriault, R.J., Bostock, H.H. 1989 Nd isotopic studies in the ca. 1.9 Ga Taltson Magmatic Zone, N.W.T. Geological Association of Canada, *Program with abstracts*, **14**: A10.
- Theriault, R.J., Ross, G.M., 1991. Nd isotopic evidence for crustal recycling in the ca. 2.0 Ga subsurface of western Canada. *Canadian Journal of Earth Sciences*, **28**: 1140-1147.
- Theriault., R.J., Tella, S., 1997. Sm-Nd isotopic study of mafic volcanic rocks from the Rankin Inlet and Tavani regions, District of Keewatin, Northwest Territories. *Radiogenic and Isotopic Studies: Report 10; Geological Survey of Canada, Current Research F* : 61-66.
- Todt, W., Cliff, R.A., Hanser, A., Hofmann., 1996. Evaluation of a ^{202}Pb - ^{205}Pb double spike for high-precision lead isotope analysis. *Earth Processes: Reading the Isotopic Code, Geophysical Monograph 95, AGU.* 429-437.
- Todt, W., Cliff, R.A., Hanser, A., Hofmann., 1996. Evaluation of a ^{202}Pb - ^{205}Pb double spike for high-precision lead isotope analysis. *Earth Processes Reading the Isotopic Code, Geophysical Monograph 95, AGU.* 429-437.
- Villeneuve, M.E., Ross, G.M., Theriault,R.J., Miles, W., Parrish, R.R., Broome, J. 1993. Tectonic subdivision and U-Pb geochronology of the crystalline basement

- of the Alberta basin, western Canada. *Geological Survey of Canada Bulletin* 447: 86p.
- Whalen, J.B., Jenner, G., Gariépy, C., Longstaffe, F. 1994. Geochemical and isotopic (Nd, O and Pb) constraints on granite sources in the Humber and Dunnage Zones, Gaspésie, Quebec, and New Brunswick: implications for tectonics and crustal structure. *Canadian Journal of Earth Sciences*, 31: 323-340.
- Williamson, J.H. 1968. Least squares fitting of a straight line. *Canadian Journal of Physics*. 46: 1845-1847.
- Windley, B.F., 1983 A tectonic review of the Proterozoic. *Geological Society of America Memoir*, 161: 1-10.
- Windley, B.F., 1992. Proterozoic collisional and accretionary orogens in *Proterozoic Crustal Evolution*, (ed) K.C. Condie, Elsevier, 419-440.
- Windley, B.F., 1995. The Evolving Continents. *John Wiley & Sons*. 526p.
- Zartman, R.E., Doe, B. 1981. Plumbotectonics -The Model. *Tectonophysics*, 75: 135-162.

APPENDIX A

Location of samples.

Sample	UTM co-ordinates <u>Northing-Easting</u>
TMZ 1	6564659-537141
TMZ 2	6561193-537132
TMZ 5	6580400-546600
TMZ 6	6583930-547450
TMZ 8	6594849-546839
TMZ 9	6599947-492374
TMZ 10	6614444-497680
TMZ 11	6619028-505881
TMZ 13	6628851-511101
TMZ 16	6641675-508880
TMZ 20	6643769-522519
TMZ 22	6644428-553663
TMZ 23	6633521-550316
TMZ 27	6619015-548322
TMZ 30	6601500-546800
TMZ 31A	6621719-456300
TMZ 33	6627207-484267
TMZ 35	6639720-443573
TMZ 36	6649999-490371
TMZ 37	6546100-492831
TMZ 38A	6546511-491937
TMZ 38B	6546511-491937
TMZ 39A	5595460-497579
TMZ 40	6574535-499598
TMZ 42	6593363-492584

APPENDIX B

The following discussion is a summary of the isotope systematics of neodymium, lead and oxygen and the ability of these systems to differentiate between crustal versus mantle signatures in granite petrogenesis. Neodymium and lead isotopes provide independent estimates of the average age of granite source regions. The oxygen isotope system provides information on proportion of supracrustal materials in the source region.

Neodymium

Samarium and neodymium are rare earth elements (REE) that occur in many rock forming silicate, phosphate and carbonate minerals. One of the isotopes of samarium (^{147}Sm) is radioactive, and decays by a emission to a stable isotope of neodymium (^{143}Nd), (Faure 1986). ^{144}Nd is used as a reference isotope as it is stable and non-radiogenic in nature since the atoms of ^{144}Nd in a unit weight of rock or mineral remains unchanged as long as the system in which it resides remains closed to Nd. As a result of this, the ratio $^{143}\text{Nd}/^{144}\text{Nd}$ of all rocks increases with time but the rate of increase depends on the degree of Sm enrichment relative to Nd. The isotope systematics of the Sm-Nd system have proven to be very useful in studying the processes of crustal evolution. The decay of ^{147}Sm to ^{143}Nd allows $^{143}\text{Nd}/^{144}\text{Nd}$ to be used to trace Sm/Nd fractionation over a long period of time and different geological processes. This is possible because the two elements are strongly fractionated in partial melting processes relating to the extraction of crust from the mantle but relatively little fractionated in inter-crustal processes. More specifically, the daughter element (Nd) is fractionated into the crust relative to the parent element (Sm). As a result of its lower elemental ratio of Sm/Nd, the Nd isotope ratio

($^{143}\text{Nd}/^{144}\text{Nd}$) of crust increases at a slower rate than does the mantle from which it was derived. In other words, when a crustal rock is extracted from the depleted mantle, the $^{143}\text{Nd}/^{144}\text{Nd}$ ratio of the depleted mantle and the partial melt will be the same, but the $^{147}\text{Sm}/^{144}\text{Nd}$ ratio will be lower in the melt. Therefore, from that period onwards the $^{143}\text{Nd}/^{144}\text{Nd}$ ratio of the mantle will increase more rapidly than that of the crystallized partial melt extracted from it (Fig 18A). So this particular isotope system has long been used as an indicator of chemical processes involved in crust formation. The Sm-Nd isotopic system, in conjunction with absolute age determinations, has been used to trace the history of light REE enrichment or depletion that accompanies the evolution of an igneous system (Faure 1986). CHUR represents the undifferentiated material that comprises the early solar system, as recorded by chondritic meteorites (Faure 1986). It is unlikely to have geological significance but provides a good reference point.

The convention of expressing Nd isotope composition of a rock at the time of its crystallization (t) is in the form of $\epsilon\text{Nd}(t)$ units defined as :

$$\epsilon\text{Nd}(t) = 10^4 \times \left[\frac{{}^{143}\text{Nd}/{}^{144}\text{Nd}_{\text{SAMPLE}}^t}{{}^{143}\text{Nd}/{}^{144}\text{Nd}_{\text{CHUR}}^t} - 1 \right]$$

where ${}^{143}\text{Nd}/{}^{144}\text{Nd}_{\text{CHUR}}^t = 0.512638 - 0.1966 (e^{\lambda t} - 1)$.

and ${}^{143}\text{Nd}/{}^{144}\text{Nd}_{\text{SAMPLE}}^t = {}^{143}\text{Nd}/{}^{144}\text{Nd}_{\text{MEAS}}^t - {}^{147}\text{Sm}/{}^{144}\text{Nd}_{\text{MEAS}} (e^{\lambda t} - 1)$.

In the above equation t=time of crystallization, $\lambda = {}^{147}\text{Sm}$ decay constant,

${}^{143}\text{Nd}/{}^{144}\text{Nd}_{\text{CHUR}}^t$ is the Nd isotopic composition of the chondritic uniform reservoir

at time t, 0.512638 is the ${}^{143}\text{Nd}/{}^{144}\text{Nd}$ isotopic composition of CHUR today, 0.1966 is

the ${}^{147}\text{Sm}/{}^{144}\text{Nd}$ of CHUR and ${}^{143}\text{Nd}/{}^{144}\text{Nd}_{\text{SAMPLE}}^t$ is the age corrected Nd isotopic

composition of the sample based on the present day ${}^{143}\text{Nd}/{}^{144}\text{Nd}$ and ${}^{147}\text{Sm}/{}^{144}\text{Nd}$

measured for the sample.

It is generally accepted that positive values of ϵ_{Nd} at the time of crystallization indicate a long term history of the light REE depletion (higher Sm/Nd) of a rock or its source relative to the chondritic reference reservoir (CHUR) whereas negative ϵ_{Nd} indicates a history of long term light REE enrichment (lower Sm/Nd) of a rock or its source relative to CHUR. In general, the Earth's upper mantle or crust newly developed from the mantle displays positive values, whereas older recycled continental crust displays lower positive or negative ϵ_{Nd} values.

Granites that formed due to continent-continent collisions typically show negative ϵ_{Nd} values, indicating derivation of these granites from crustal source rocks (Fig 18C). In contrast, granites or volcanic rocks formed in subduction zones show positive to weakly negative ϵ_{Nd} values, reflecting significant mantle-derived component to these magmas with variable amounts of crustal contamination. For example Fig 18C shows two granites a and b, formed 3 b.y ago. When their present day ϵ_{Nd} values are recalculated to obtain their initial ϵ_{Nd} values at the time of crystallisation, then granite a had ϵ_{Nd} value close to that of the depleted mantle, indicating a large amount of mantle contribution to these granites; whereas granite b using the same principle has strong negative ϵ_{Nd} values indicative of derivation of a source rock with a long crustal residence time.

Lead

Lead on Earth consists of primeval lead (present when the Earth formed 4.55 Ga ago) plus radiogenic lead derived from radioactive decay of uranium and thorium. Three isotopes, ^{206}Pb , ^{207}Pb , ^{208}Pb , form from the radioactive decay of ^{238}U , ^{235}U and ^{232}Th , respectively, while a fourth isotope ^{204}Pb is non-radiogenic. The bulk

continental crust has higher U/Pb and Th/Pb than the mantle. Therefore, the Pb isotopic composition of the crust evolves differently with time than the mantle from which it was derived (Fig 19A).

The geochemical behavior of U-Pb in the crust is different than the Sm-Nd system. This is due to the fact that U and Pb are more mobile than the REE elements during crustal processes of weathering, alteration and metamorphism. These processes typically change the primary U/Pb ratios of rocks. As a result of this, a back calculation of initial Pb isotopic composition from present-day (measured) Pb isotope ratios of whole rocks is problematic. Such a calculation is possible in the Sm-Nd system because of the immobility of Sm and Nd in crustal processes. In order to circumvent this problem, initial Pb isotope composition of granites are determined from strongly leached alkali feldspars. Since the U/Pb and the Th/Pb ratios in alkali feldspars are very low, only a marginal amount of extra radiogenic lead is formed in the rock subsequent to crystallization. Thus, the alkali feldspars preserves a record of lead isotopic composition of the magma from which it is crystallized. The alkali feldspars are leached in order to remove any radiogenic Pb present in fractures, and to obtain the non-radiogenic Pb present in the mineral structure.

Oxygen

The fundamental difference between radiogenic and stable isotope systems, are that the former provides a monitor of time-dependent processes whereas the latter provide a monitor of time-independent but temperature-dependent processes. Oxygen is probably the most widely used stable isotope system.

Oxygen isotope compositions are denoted in $\delta^{18}\text{O}$ notation where

$$\left(\frac{R_{\text{SAMPLE}}}{R_{\text{STANDARD}}} - 1\right) \times 1000$$

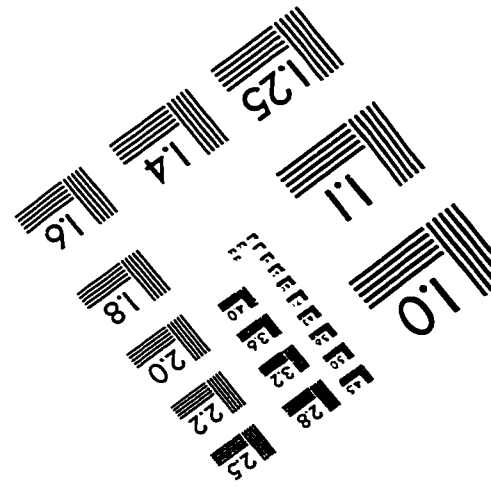
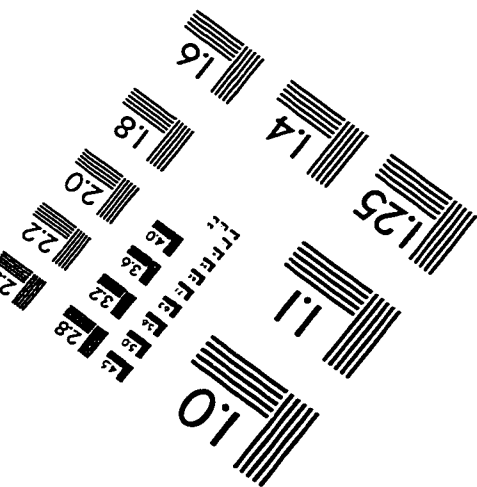
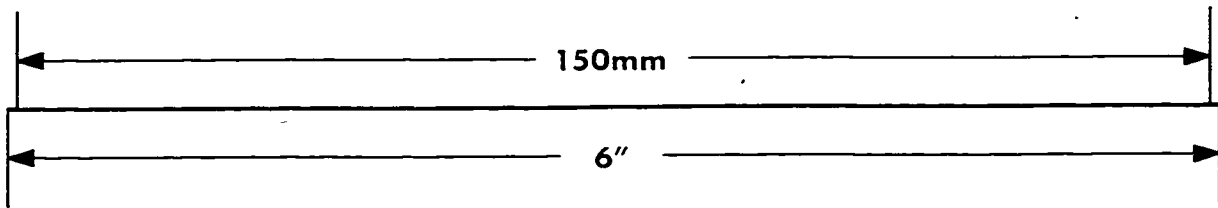
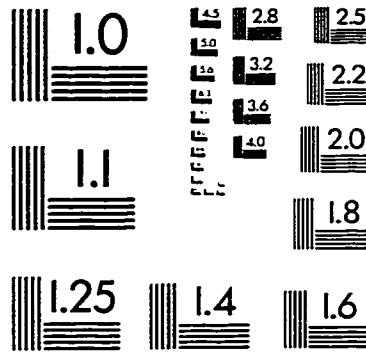
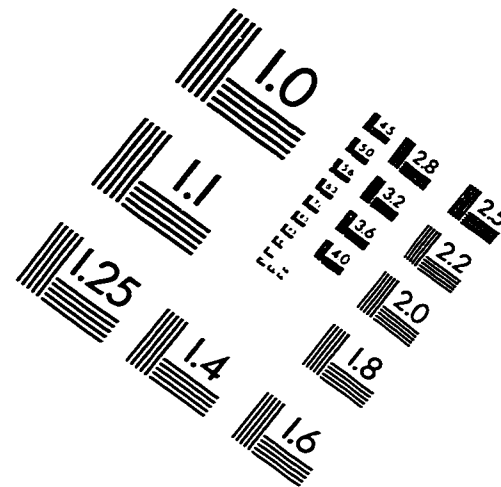
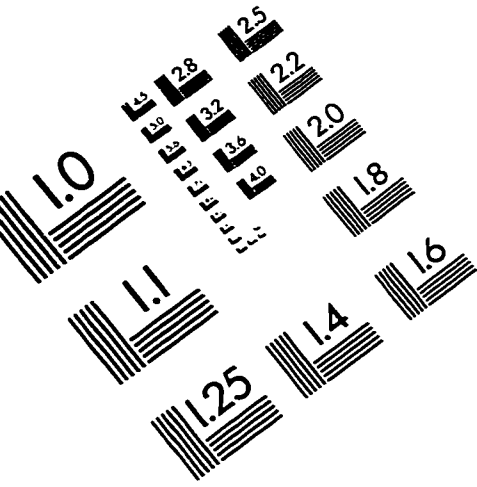
and $R = (^{18}\text{O}/^{16}\text{O})$.

In general distribution of stable isotopes between coexisting phases A and B are in terms of a fractionation factor α_{A-B} where $\alpha_{A-B} = R_A/R_B$. For numerical convenience the fractionation factor is often expressed in terms of $\Delta_{A-B} = 1000 \ln \alpha_{A-B}$

The $\delta^{18}\text{O}$ values of crustal rocks are generally higher than mantle-derived rocks. This is because some crustal rocks have protoliths that had a prehistory of water-rock interaction at low temperatures. For example if mantle-derived rocks (+5.5‰) interacted with ocean water (0‰) at 25°C, the whole rock-water fractionation factor at that temperature would cause the basalts to be enriched in ^{18}O , upto $\delta^{18}\text{O}$ values of 12‰. Similar or even higher $\delta^{18}\text{O}$ values are produced during processes of weathering, erosion and sedimentation in the crust. This is reflected in high $\delta^{18}\text{O}$ values for sediments or their metamorphosed equivalents.

If these altered volcanic rocks or metasedimentary rocks are buried by tectonic processes, they become potential source rocks for the generation of granitic magmas. The magmas, in turn, mimic the isotopic composition of their sources. Hence granites derived exclusively from the crust will typically have higher $\delta^{18}\text{O}$ values than granites derived from a combination of crustal and mantle source rocks (Fig 19B)

IMAGE EVALUATION TEST TARGET (QA-3)



APPLIED IMAGE . Inc
1653 East Main Street
Rochester, NY 14609 USA
Phone: 716/482-0300
Fax: 716/288-5989

© 1993, Applied Image, Inc., All Rights Reserved